Journal of South American Earth Sciences 29 (2010) 327–345

Contents lists available at ScienceDirect

Journal of South American Earth Sciences

journal homepage: www.elsevier.com/locate/jsames

Sedimentological, geochemical and paleontological insights applied to continental omission surfaces: A new approach for reconstructing an eocene foreland basin in NW Argentina

C. del Papa [a,*], A. Kirschbaum [b], J. Powell [c], A. Brod [d], F. Hongn [a], M. Pimentel [d]

[a] CONICET – Universidad Nacional de Salta, Buenos Aires 177, 4400 Salta, Argentina
[b] CONICET – IBIGEO, Museo de Ciencias Naturales, UNSa, Mendoza 2, 4400 Salta, Argentina
[c] CONICET-UNT, Miguel Lillo 205, 4000 Tucumán, Argentina
[d] Universidade de Brasília, Campus Universitário Darcy Ribeiro, Asa Norte, 70.910-900 Brasília, DF, Brazil

ARTICLE INFO

Article history:
Received 23 December 2008
Accepted 8 June 2009

Keywords:
Omission surface
Paleosols
Geochemistry
Eocene foreland basin
South America Land Mammal Ages
Northwestern Argentina

ABSTRACT

An Eocene foreland basin linked to the Andean uplift in northwestern Argentina has recently been proposed. The basin is divided and partially eroded due to subsequent Neogene orogenic phases, so that a simple reconstruction is insufficient to describe complex field relationships. This presents a new challenge in understanding the initial phases of Central Andean evolution. We propose a multidisciplinary approach in key locations and/or at key geological features as a way to reconstruct the Paleogene basin. In this contribution, we report on sedimentological and geochemical evidence of a conspicuous weathering surface in the continental Eocene Lumbrera Formation and provide an age estimate based on vertebrate mammalian biostratigraphy and an absolute U/Pb zircon age of 39.9 Ma. Weathering surfaces become evident when diagnostic features like paleosols, karsts, and trace fossils are distinctive but, in our case, these characteristics only emerge through detailed sedimentological and geochemical surveys. The Lumbrera paleosurface is represented by a hardened level (20–30 cm thick) characterized by moderately developed reddish paleosols. Moreover, major and trace element profiles show inflections at the top and/or base of the weathered horizon delineating it. A modified form of the chemical index of alteration shows that chemical leaching was moderate and not extensive. In addition, mammalian fossil records substantially differ below and above the weathered paleosol-bearing surface. We conclude that this horizon represents a Middle Eocene omission surface and represents a key level marking a major basin change in northwest Argentina, adding a new constraints for Eocene foreland reconstruction.

ARTICLE INFO

Article history:
Received 23 December 2008
Accepted 8 June 2009

Palabras clave:
Superficie de omisión
Paleosuelos
Geoquímica
Antepaís eoceno
Edades Mamíferos Sudamericanos
Noroeste argentino

RESUMEN

Recientemente se ha propuesto la existencia de una cuenca de antepaís eocena en el noroeste argentino. Esta cuenca está actualmente dividida y parcialmente erosionada como consecuencia de las subsecuentes etapas de deformación neógenas; esta deformación produjo complejas relaciones de campo que dificultan su reconstrucción, lo que constituye un nuevo desafío para el conocimiento de las etapas iniciales de formación de los Andes Centrales. Se propone un enfoque multidisciplinario en localidades clave y/o en estructuras geológicas clave como método para reconstruir esta cuenca paleógena. En esta contribución damos a conocer una conspicua paleosuperficie de meteorización en la Formación Lumbrera (Eoceno) a través de evidencias sedimentológicas y geoquímicas. Asimismo se aportan datos bioestratigráficos de vertebrados y una edad absoluta (U/Pb circón) de 39,9 Ma para esta secuencia. Las superficies de meteorización resultan evidentes cuando presentan rasgos diagnósticos como paleosuelos, karsts y asociaciones de trazas fósiles, pero en nuestro caso las evidencias surgieron sólo a través del estudio sedimentológico y geoquímico de detalle. La paleosuperficie de la Formación Lumbrera está formada por un nivel endurecido de 20-30 cm de espesor caracterizado por el desarrollo moderado de paleosuelos rojizos. Asimismo la distribución de elementos mayoritarios y trazas muestran inflexiones tanto al tope como a la base del nivel endurecido, demarcándolo. El índice de alteración química (CIA) empleando una

* Corresponding author. Fax: +54 3874318086.
E-mail addresses: delpapacecilia@yahoo.com (C. del Papa), alikir2003@yahoo.com.ar (A. Kirschbaum), powell.jaime@gmail.com (J. Powell), brod@unb.br (A. Brod), fhongn@aol.com (F. Hongn), marcio@unb.br (M. Pimentel).

0895-9811/$ - see front matter © 2009 Elsevier Ltd. All rights reserved.
doi:10.1016/j.jsames.2009.06.004

fórmula modificada, indica que la meteorización fue de orden moderado. Por otra parte, el registro de fósiles de vertebrados difiere sustancialmente por abajo y por arriba del nivel meteorizado. Concluimos que este horizonte constituye una superficie de omisión de edad Eoceno medio y representa una superficie clave que divide las cuencas eocenas, brindando nuevas evidencias para la reconstrucción de la cuenca de antepaís en el noroeste de Argentina.

1. Introduction

Foreland basin systems originate as a consequence of flexural depression of the lithosphere in response, among other factors, to the tectonic loading of an orogenic wedge (Jordan, 1981; Allen and Allen, 1990; Catuneanu, 2004).

In simple retroarc foreland models while the deformation progresses the basin becomes dissected provoking the cannibalization and recycling of it own deposits and the depozones migrate in the cratonward direction (Fleming and Jordan, 1989; Allen and Allen, 1990; Sinclair et al., 1991; Horton and DeCelles, 1997). In ancient complex foreland systems this scenario turns more complicated and difficult to identify due to, among other reasons, the incomplete stratigraphic record (e.g. Horton, 1998) and the presence of pre-existing heterogeneities which could have conditioned basin evolution favoring structural fragmentation where local depozones could develop (Jordan and Allmendinger, 1986; DeCelles and Giles, 1996; Jordan et al., 2001). This is the case of the Eocene-present day Andean foreland of the Eastern Cordillera of northwest Argentina which developed, in part, superimposed to the Cretaceous rift basin (Fig. 1A) conditioning the style and the propagation of the deformation because of the reactivation of normal faults (Grier et al., 1991; Coutand et al., 2001; Carrera et al., 2006; Mortimer et al., 2007; Hongn et al., 2007). Additionally, Riller and Hongn (2003) and Hongn et al. (2007, 2008) pointed that, in addition to normal faulting the presence of Proterozoic and lower Paleozoic

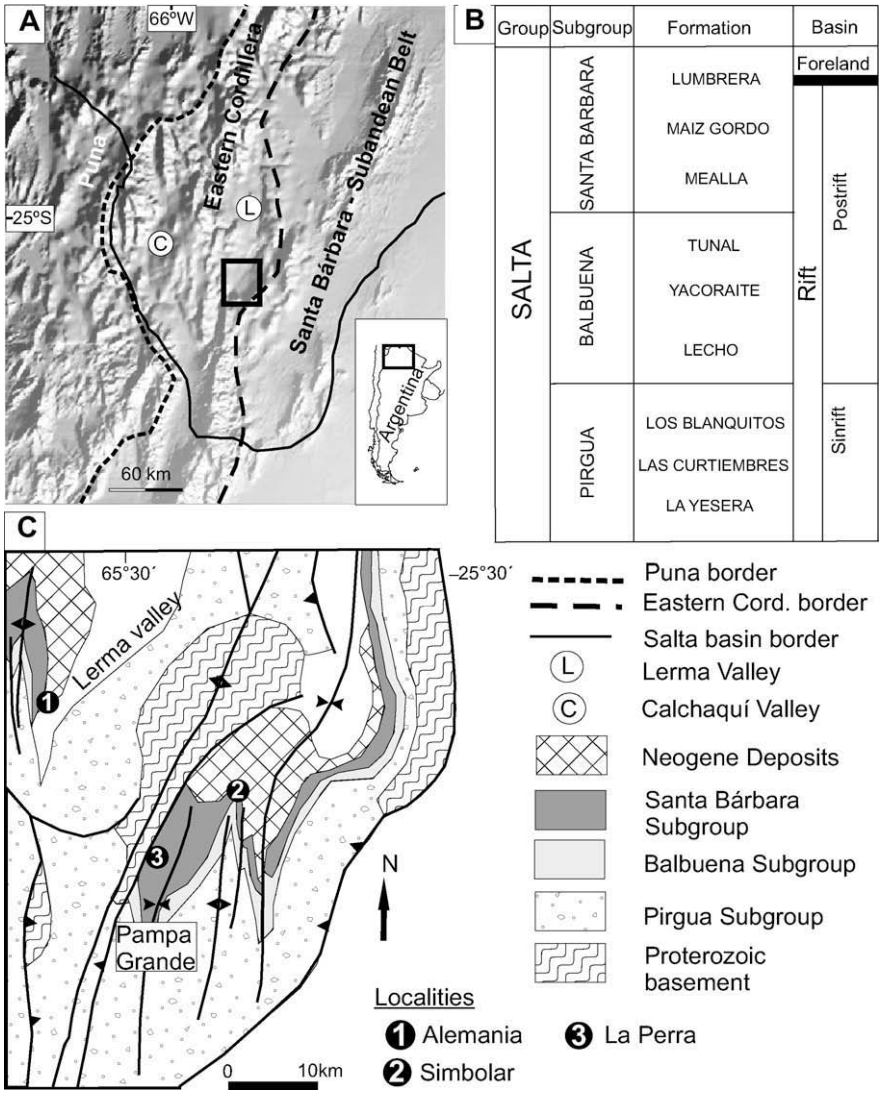

Fig. 1. (A) Central Andes of northwestern Argentina, studied area shown. (B) Stratigraphic chart of the Salta basin. (C) Geological map of the Lerma valley and Pampa Grande region (based on Mon, 2001).

basement heterogeneities (e.g. dykes, foliation, shear zones) plays a role in foreland system development.

The Andean foreland history is better known from the Miocene to present day than before this time interval (Jordan and Alonso, 1987; Kley, 1998; Galli and Hernández, 1999; Reynolds et al., 2000; Echavarría et al., 2003; Coutand et al., 2006; Carrera and Muñoz, 2008) than the previous history. A complex Eocene foreland basin has recently been proposed (Hongn et al., 2007; Carrapa and DeCelles, 2008) as alternative to a rather simple Paleogene foreland basin previously postulated (Boll and Hernández, 1986; Jordan and Alonso, 1987; Vergani and Starck, 1989; Starck and Vergani, 1996).

The Eocene time of northwestern Argentina records complex basin and structural evolution, including continental sedimentation of the post-rift Salta Basin (Fig. 1B) (see Salfity and Marquillas, 1994 and Marquillas et al., 2005 for a regional account) and the beginning of the Andean uplift and foreland system evolution (Fig. 1B) (Coutand et al., 2001; Haschke et al., 2005; Hongn et al., 2007; DeCelles et al., 2007).

Starck and Vergani (1996), Hernández et al. (1999), and Carrapa and DeCelles (2008), among others, based on structural and sedimentological data, have proposed that part of the eastern Puna and the Puna – Eastern Cordillera transition – Valle Calchaquí – (Fig. 1A) would represent the wedge-top depozone. Although this proposal represents a first step to clarify the Eocene scenario, the overall geometry of the basin and the original spatial relation between the thrust faults and the basin (e.g., where were the foredeep and forebulge located, and also what was the structural style of this early stage of deformation?), are all currently unresolved questions.

In this contribution we focus in the Lerma valley, located approximately 70 km from the interpreted wedge top depozone (Fig. 1A) where no evidence of Eocene deformation is recorded. We investigate the stratigraphy to determine the sedimentological expression of the basin shift from the Eocene rift to Eocene foreland through sedimentological, geochemical and vertebrate paleontological studies of the Lumbrera Formation. Also a new U/Pb date allows better constraints on the beginning of Andean evolution. Our studies allow the identification of a paleoweathering surface interpreted as a continental omission surface and we discuss its meaning in the context of Eocene basin evolution. We conclude that this regional paleosurface represents a key level and marks a major basin change in northwest of Argentina, adding a new constraints for Eocene foreland reconstruction.

2. Stratigraphy and geological setting

The studied area is located in the southern Eastern Cordillera of northwest Argentina coincident with the transition area where the subduction angle of the subducting Nazca plate progressively changes (Cahill and Isacks, 1992), characterized by thick-skinned and thin-skinned structural styles (Jordan and Allmendinger, 1986). Moreover the area between 24°LS and 26°LS represents the southern and western ends of the mechanical Salta rift basin (Salfity and Marquillas, 1994; Sabino, 2004), where the superimposed foreland is placed (Fig. 1A and B). This scenario evidences that the transformation of one basin into another and the history of deformation and basin subsidence were complex (Coutand et al., 2001; Mortimer et al., 2007; Hongn et al., 2007).

To analyze this basin passage and its characteristics in the Lerma valley (Fig. 1C) we describe the sedimentary settings of the Eocene Lumbrera Formation and, in particular, we analyze in detail the indurated paleosurface identified in this unit.

Lumbrera is the upper Formation of the Salta Group (Fig. 1B), with infill deposits of an extensive rift basin – Salta Group – developed in northern Argentina (Fig. 1A) during the Neocomian to Eocene (Salfity, 1982; Salfity and Marquillas, 1994). The Salta Group consist of synrift coarse-grained alluvial deposits (Pirgua Subgroup) and postrift fine-grained to chemical deposits (Balbuena and Sánta Bárbara Subgroups; Fig. 1B) (Marquillas et al., 2005).

Based on seismic section interpretation (Monaldi et al., 1993) and on paleoenvironments and facies distribution of the Lumbrera Formation (del Papa, 2006) a paleogeographic change modifying the locations of the main depocenters has been interpreted. This change was attributed to the beginning of foreland basin. Besides, based on distinctive and contrasting sedimentary environments, Gómez Omil et al. (1989) and lately del Papa (2006) divided this unit into two subunits: lower Lumbrera and upper Lumbrera (Fig. 2A).

In the Lerma valley and Pampa Grande region (Fig. 1C), the Lumbrera Formation consists of 300–500 m of intercalated red fine-grained sediments and sandstones (Fig. 2A).

In this area, lower Lumbrera consists of moderately sinuous fluvial facies associated with perennial freshwater lake deposits known as "Faja Verde" (Schlagintweit, 1936), and including the Faja Verde I and the Faja Verde II levels described in Pampa Grande region by Carbajal et al. (1977).

The fluvial system is integrated by the association of bar complex channel-fill facies, levee and floodplain fines. The channel-fill facies consists of cross-stratified and laminated coarse- to fine-grained sandstone with well-defined lateral-accretion bars structures. Ribbon-like laminated siltstones and fine sandstones associated to channels facies represent levee deposits. Floodplain facies consist of laterally continuous sheets of reddish siltstones and sandstones with paleosols levels. Laterally, deltaic facies of Gilbert type developed and interfingered with lacustrine facies. The lacustrine deposits range in thickness between 82 m in Alemania and 114 m in Simbolar and are characterized by greenish to dark gray colors of fine-grained sediments (Fig. 2B). In the littoral zones are represented by medium to fine-grained sandstones and siltstones with lenticular to wavy bedding structures and wave-rippled lamination. Besides, fine laminated mudstones and siltstones with high organic content characterized inner lake deposits.

On the other hand, the upper Lumbrera consists of sandy fluvial deposits associated with an ephemeral clastic lake (del Papa, 2006). The fluvial system is integrated by sandstone beds filling shallow channels. Normal grading, both tabular and trough cross-bedding and dish structures characterize the fluvial channels. Thick, reddish siltstones and fine-grained sandstones (Fig. 2C) with some levels of calcrete paleosols represent floodplain deposits interstratified with channel deposits. Lacustrine deposits are characterized by laminated siltstones, sheet-like sandstones with wave-rippled lamination and red massive siltstones with gypsum/anhydrite nodules, indicating extensive saline mud-flat to shallow lakes (del Papa, 2006).

The contact between the lower and upper sub-units of the Lumbrera Formation is abrupt and represented by an indurated and crusted level (Fig. 2D) traceable through 500 km^2, extending through part of the Lerma valley and the nearby Pampa Grande region (Fig. 1C). The indurated level was affected by weathering over an extensive desiccation surface on the Faja Verde lake, and was, as inferred from geological attributes, a nearly flat surface.

3. Materials and methods

We studied three detailed stratigraphic sections: Alemania, Simbolar and La Perra (Fig. 1C), describing the lithology, color, and sedimentary and pedologic structures through the indurated surface. Decimeter-spaced sampling took into consideration outcrop-scale physical changes, for example of color and structures.

Each sample was petrographically studied in thin section to evaluate soil micromorphological features. X-ray diffraction from

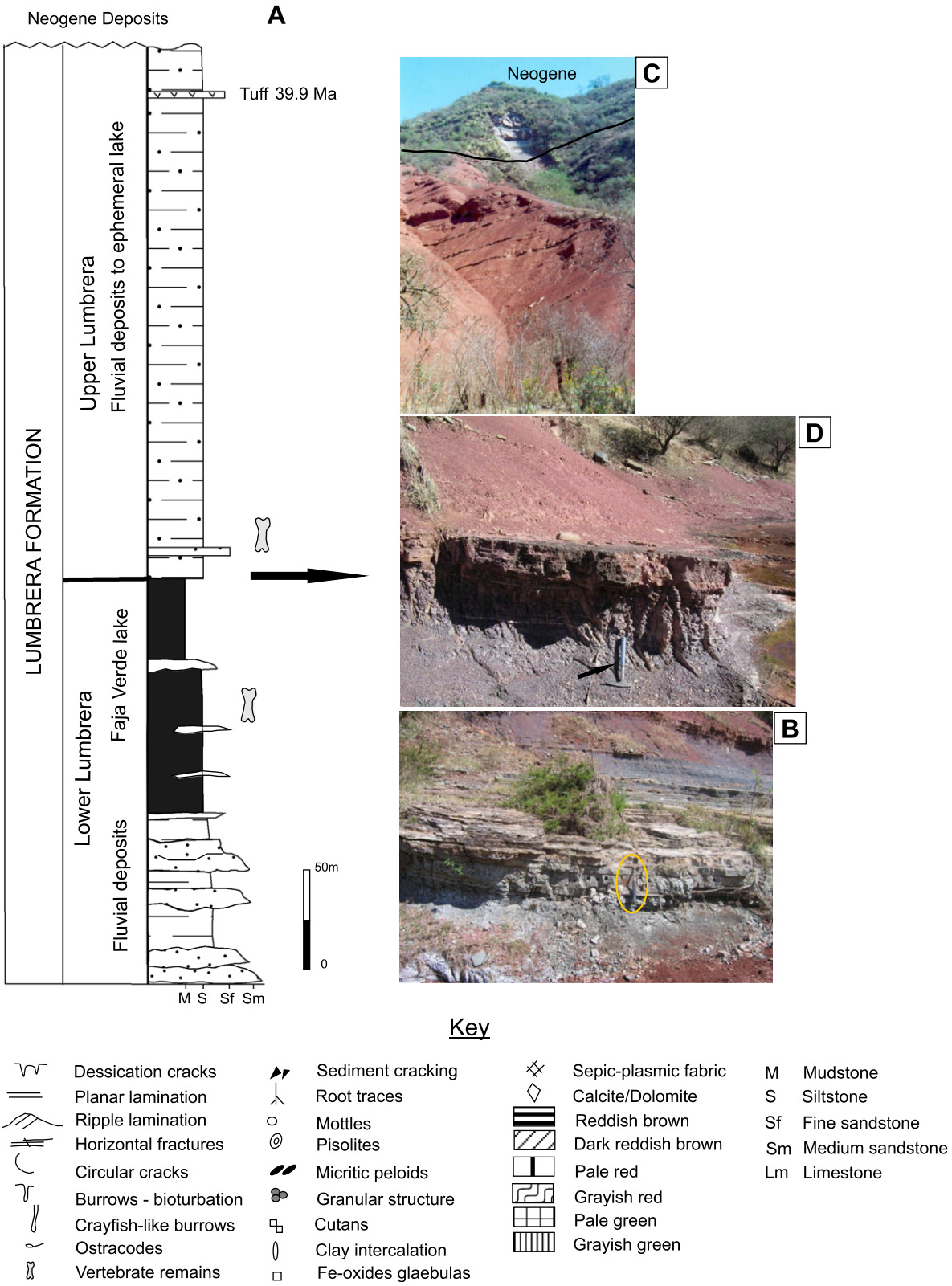

Fig. 2. (A). Lower and upper Lumbrera log showing the main sedimentary environments and the stratigraphic position of the vertebrate fossils, as well as the volcanic tuff in Simbolar. (B) Lacustrine facies of the Faja Verde lake of lower Lumbrera. (C) Thick siltstones packages with sheet-like sandstones interbedded of upper Lumbrera (outcrop is 70 m thick). (D) Indurated level marking the contact between the lower and upper Lumbrera (hammer for scale).

both whole-rock and clay sub-samples (<2 μm; 27 samples) were performed with a Rigaku Denki, D/Max II-C diffractometer (Lanais, Salta University) with Cu Kα radiation operated at 40 mA and 30 kV. Clay minerals were identified according to the position of the (0 0 l) series of basal reflections on XRD patterns of air-dried, ethylene-glycolated, and heated (at 550 °C for 2 h) specimens.

In addition, major and trace-element XRF analyses were carried out at the Lanais (Salta University) in order to recognize

and evaluate chemical changes of the parent material. The analyses were performed using a WDS Rigaku 2000 spectrometer equipped with a Rh tube, SC detector, and PC gas flow. The analyzing monochrome crystals were LIF, PET, TAP, and GE. Each sample was first ground in a Hersog-type tungsten carbide mill and dried at 105 °C for 24 h. Loss on ignition was determined at 950 °C until the sample reached a constant weight. Major elements were analyzed on Lithium Tetraborate anhydrous fusion discs prepared with a sample/flux ratio of 1/6. Trace elements were analyzed on pressed pellets prepared with elvacite/acetone, (20/80) at 1.400 kg/cm^2. The quantification curves were compared with standard rock calibrations: major elements, JG-2, JG-3, JA-3, JA-2, JB-3, JP-1, JR-2, JF-2 (Geological Survey of Japan); SDC-1, SCO-1, BIR-1 and W-2., DNC-1 STM-1 (United States Geological Survey) and minor elements, JGB-1, JR-2, JB-3, JF-2, JG-3, JA-2, JG-2, JP-1 (Geological Survey of Japan). SCO-1, DNC-1, SGR-1, W-2, BIR-1, SDO-1, G-1, AGV-1, W-1, G-2, PCC-1, GSN, BE-N (United States Geological Survey); AN-G (Grupe International deTravail / International Working Group); GA, GH, BR (Centre de Recherches Petrographique et Geochimiques); DRN, DTN, UBN, FKN (Association National de la Recherche Technique); SY2 (Canadian Certified Reference Material Project).

U/Pb dating was performed in zircon grains; zircon concentrates were extracted from ca. 10 kg rock samples, using conventional gravimetric (DENSITEST) and magnetic (Frantz isodynamic separator) techniques at the Geochronology Laboratory of the University of Brasilia. Final purification was achieved by hand picking using a binocular microscope. Zircon fractions were dissolved in concentrated HF and HNO_3 ($HF:HNO_3 = 4:1$) using microcapsules in Parr-type bombs. A mixed ^{205}Pb–^{235}U spike was used. Chemical extraction followed standard anion exchange techniques, using Teflon microcolumns, following procedures modified from Krogh (1973). Pb and U were loaded together on single Re filaments with H_3PO_4 and Si gel, and isotopic analyses were carried out on a Finnigan MAT-262 multi-collector mass spectrometer equipped with secondary electron multiplier ion counting at the Geochronology Laboratory of the University of Brasilia. Procedure blanks for Pb, at the time of analyses, were better than 15 pg. PBDAT (Ludwig, 1993) and ISOPLOT-Ex (Ludwig, 2001) were used for data reduction and age calculation.

The paleontological material mentioned and considered in this article is deposited at the collections of the Museum of La Plata (La Plata, Buenos Aires) and the Instituto Miguel Lillo (Tucumán University).

4. Indurated paleosurface and paleosol

4.1. Alemania locality (site 1 of Fig. 1C)

At this locality a conspicuous, 25 cm-thick indurated section was identified (Fig. 3A). Desiccation cracks occur all along the crusted surface. The polygons are 10–15 cm and the wedges penetrate into the sediments few millimeters (Fig. 3B). The wedges are filled with red silty and sandy material from the overlying sediments.

Distinctive changes in color from the top of the paleosol downward characterize it. From pale red (10R 6/2) color grades to brownish gray (5YR 4/1, 10R 4/2) and further down the profile to grayish green (10GY 5/2) and grayish green (10G 4/2), the latter colors typical of the unaltered lacustrine parent material (Fig. 3A). These changes in color are coincident with paleosols horizons. The uppermost horizon is characterized by a pinkish-white, well-laminated 2 cm thick sand-rich bed with ripple laminations (Fig. 3C and D – IVd level). The middle horizon is reddish-gray, wacke to arkose, 5–6 cm thick, in which slight and discontinuous primary lamination is preserved, millimeter-scale granular aggregations interpreted as granular ped structures (Fig. 3E) were identified. This horizon is densely rooted (Fig. 3C – IVc level); the roots are recognized by their taper and downward branching features (Retallack, 1988). They are typically isolated filamentous-like, ranging from 1 to 4 cm long and 1–2 mm in diameter. The roots consist of an individual vertical stem with minor lateral offshoots. The central tubular feature is filled with fine-grained material (clay and silt) darker than the surrounding groundmass; and in others, calcite crystals fill the voids. The lowest horizon is red to greenish-gray, sandy siltstone, 4–5 cm thick, where no primary lamination is recognized (Fig. 3C – IVb and IVa levels). The passage from the sandy rooted to siltstone levels is clear and wavy (Retallack, 1988) (Fig. 3F). Also in this horizon some root casts and granular peds are preserved with the same characteristics of the upper one; moreover, platy claystone intraclasts parallel to stratification were also identified.

Based on the lighter color, coarser textures of the underlying beds, the IVc level is interpreted as an eluvial (E) horizon, while the IVa and IVb levels are interpreted as illuvial (Bt) horizon (Fig. 3F). The uppermost bed (IVd level) is very weakly modified by pedogenesis, indicating a sporadic increment in the sedimentation rate (Fig. 3C and D). This level is considered here as a cumulative horizon (Birkeland, 1984).

Animal burrows were recognized in the three horizons, comprising simple tubular features with constant diameter. They are circular in cross-section and filled with the matrix material (red siltstone and disseminate sandy grains) and calcite (crystal tubes); backfill structures are common. Two types are distinguished: (a) minor horizontal to vertical burrows 1–2 mm wide and a few centimeters long; in some cases the sediments are only disturbed, generating biodeformation features and (b) greater vertical burrows, 8–10 mm wide (Fig. 3B) and many centimeters long. In some cases, it was possible to observe the presence of a thin wall coating the burrow tube.

Based on petrographic and polished hand-sample observations, minor burrows (a) crosscut and are cut by roots, suggesting that burrowing was contemporaneous with soil-forming processes. On the other hand, bigger burrows (b) cut both minor burrows and root traces; no observations in the opposite sense were made. The latter burrows (b) resemble crayfish traces, both in size and wall presence (Hasiotis and Mitchell, 1993), and postdate soil development.

Eight samples of representative decimeter-long sections were collected below, across, and above the weathered surface (Fig. 3A). Fig. 3G shows the main minerals identified in the whole rock. Illite is the only abundant clay, although traces of smectite were also detected.

Petrographic studies indicate that the uppermost cumulative horizon is an arkose with granular fabric and Fe-oxides coating the skeleton grains and sparitic cement (Fig. 4A). Downward the profile E horizon became an arkosic wacke to sandy siltstone with intertextic microfabrics (Fig. 4B). Plasma infilling the intergranular spaces are clinobimasepic and skelsepic types (Fig. 4C). Weakly laminated to well-laminated clay-Fe line coating voids and along trace roots (Fig. 4D) are common features. Anisotropic clay coating is characterized by yellowish brown to dark reddish brown laminated material along a root trace (Fig. 4E). Clay coating suggests formation by illuviation (Brewer, 1976), in our case, microlaminated clay coating lining and filling voids clearly suggest illuvial processes (Brimhall et al., 1991; McCarthy et al., 1999).

In the silty Bt horizon there are local concentrations of a specific mineral or chemical composition that constitute accretionary bodies or glaebules (Teruggi and Andreis, 1971). Two main types of glaebules, ferruginous and calcareous, are recognized in this study, but clay concentrations also occur. Some glaebules without any visible internal lamination are nodules mainly ferruginous; but

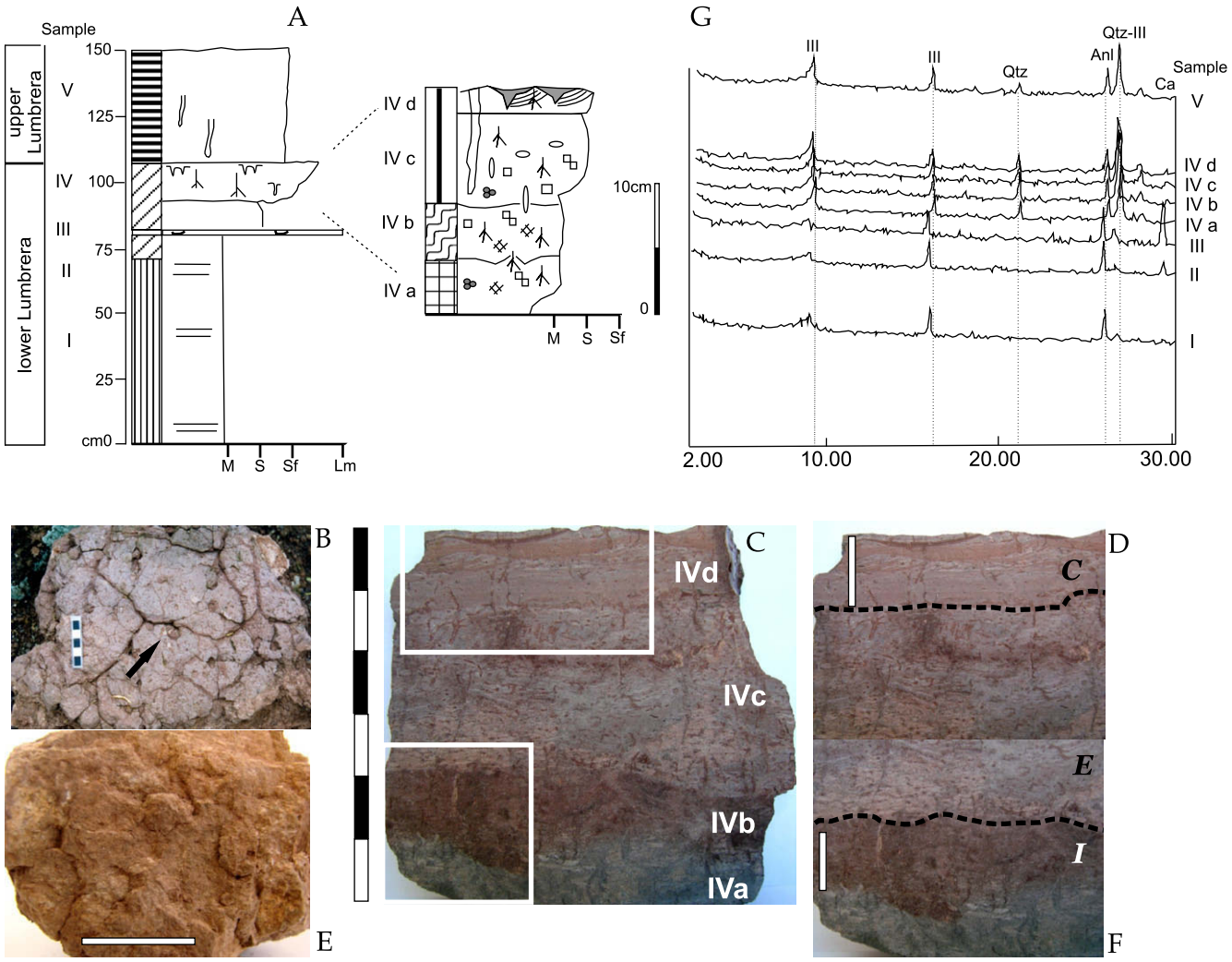

Fig. 3. (A) Alemania detail log, showing the main sedimentological and pedologic characteristics of indurated level. (B) Desiccation cracks over the paleosurface. Arrow shows crayfish-like trace fossils, Alemania (scale bar, 5 cm). (C) Polished section showing changes in color and filamentous root traces, Alemania (scale bar is 12 cm), gray pictures show the positions of D and F figures. (D) Aspect of the sandy eluvial horizon rich in root traces and the overlying cumulative "C" horizon with rippled lamination preserved; note crayfish-like trace cutting the structures (scale bar is 2.5 cm). (E) Granular pedogenic structure (scale bar, 2 cm). F. Wavy contact between sandy eluvial (*E*) and clayey illuvial (*I*) horizons (scale bar is 2.5 cm). (G) Stratigraphic variation in mineralogical composition and relative abundance from XR diffractometry.

carbonate nodules are also observed. Moreover, ferruginous concretions (concentric internal laminations) also occur (Fig. 4F) indicating seasonal growth (Ettensohn et al., 1988).

4.2. Simbolar locality (site 2 of Fig. 1C)

A 1 m-thick weathered section of siltstones and mudstones was observed here (Fig. 5A). The uppermost 12 cm are completely indurated and capped by a continuous firm crust (3 cm thick). The main features are mudcracks, burrows and root traces. These features decrease in abundance from top to the base of the indurated section. The desiccation cracks form polygons of 10–15 cm in plan view and the wedges penetrate up to 6 cm filled with red silty and sandy material from the overlying sediments.

The upper crust level is characterized by strong dark reddish brown (10R 3/4) to grayish red (5R 4/2) colors changing downward to the grayish green (10 GY 5/2) unaltered material. Neither soil structures nor horizonation were identified in outcrops; but clear bioturbation, brecciation, and mottling were observed. Some bioturbations consists of simple vertical to inclined and horizontal tubes many cm long and 1 cm to 5 mm wide filled with darker fine-grained material; interpreted as animal burrows. Other bioturbation structures have clear wedge-shapes and downward bifurcation and are interpreted as originated by root action. Fe-depleted haloed zones consisting of concentric lamination of gradational contacts of grayish red (5R 4/2) color in the inner zone to moderate yellow (5Y 7/6) to moderate reddish brown (10R 4/6) in the outer zone are also common.

We collected 12 samples from the underlying unaltered material through the weathered horizon to the overlying unaltered upper Lumbrera unit (Fig. 5A). The mineralogy determined for this section is as follows (Fig. 5B): calcite, analcime and hematite are present in all samples, whereas ankerite occurs only in the indurated horizon. Calcite and minor amounts of dolomite crystal rhombs are disseminated in the groundmass and filling cavities. Quartz, although always present, is more frequent in the upper Lumbrera Formation (see Fig. 5B), but coarser clastic feldspars and zircon grains are also noted. Illite is the only clay mineral identified.

The micromorphology suggests alteration and burrowing by organic activity, whereby the plasma is of the asepic type (argillasepic). From the uppermost level (including the upper crust)

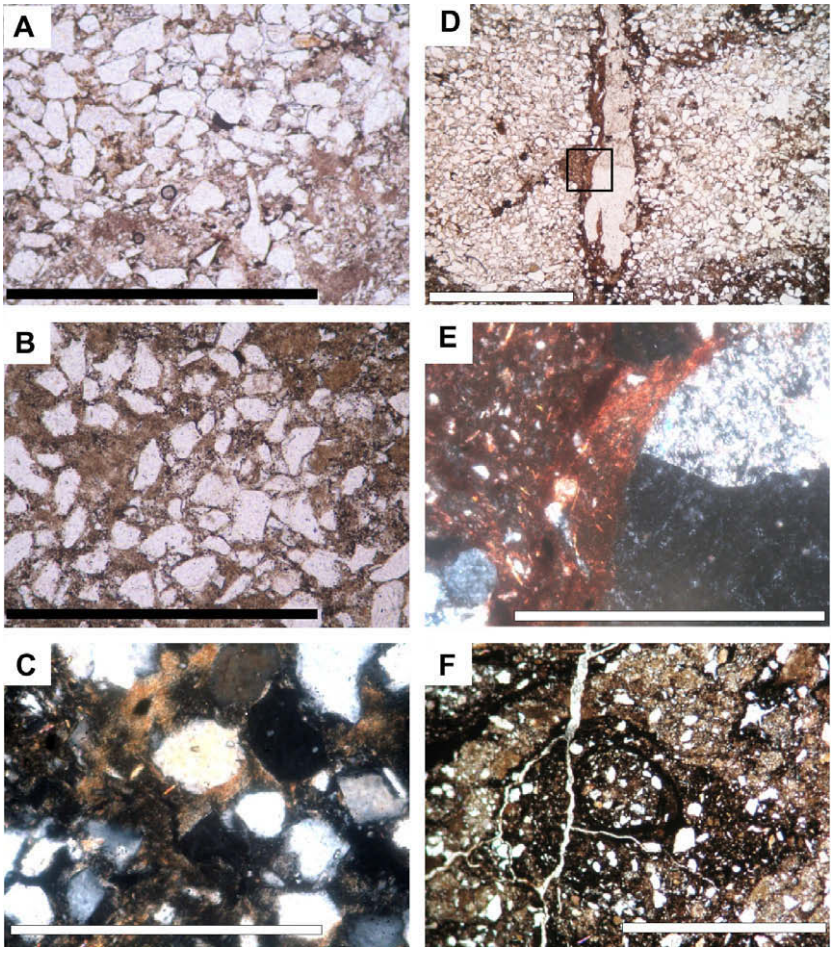

Fig. 4. Photomicrographs of paleosol micro-structures. (A) Granular (up) to intertextic (bellow) microfabric in eluvial horizon, Alemania (plane light). (B) Intertextic fabric of illuvial (Bt) horizon, Alemania (plane light). (C) Clinobimasepic plasmic fabric in illuvial horizon, Alemania, (crossed polarized light). (D) Root traces filling with sparry calcite and Fe-clay coating the root wall emplaced in granular fabric of eluvial horizon, Alemania (plane light). (E) Detail of the offshoot (square area in D) showing the microlaminated anistrotropic Fe-clay coating, Alemania, (crossed polarized light). (F) Ferruginous spherical concretion indicating seasonal growth, Simbolar (plane light). Scale bar is 1 mm except for E and C in which it is 0.5 mm.

downwards (samples 8, 7, and 6) display clotted micritic texture (Fig. 6A); this texture has been interpreted as a product of dense packing of micritic peloids (Esteban and Klappa, 1983).

Massive Fe-oxides coating voids are very common, draping circular tubes and plane and irregular voids; the contact are both diffuse and sharp with the groundmass. Also glaebules of massive Fe-oxides and peloids characterize this profile. Glaebules of calcite crystals are very common in the upper levels infilling cavities and as diffuse masses in the groundmass. Incipient blocky peds occurring as patches delineated by Fe-oxides films have been identified in this locality (Fig. 6B).

Another distinctive feature at Simbolar is the presence of horizontal to sub horizontal fractures filled with displacive sparry calcite, and extending laterally for decimeters to meters. These comprise many parallel to nearly parallel horizontal fractures, connected by subordinate vertical fractures, delineating an anastomosing pattern. Apertures range between 1 and 3 mm (open type) and the lateral extent is one centimeter to 1 m (Reichenberger, 2004), infilled with mosaic of sparry calcite (Fig. 6C). Retallack (1991) described a pervasively displacive microstructure for the Miocene paleosols of Kenya. He interpreted this structure as result of processes that produce volume changes during initial subaerial leaching and cementation in pyroclastic parent material; being this process more effective under humid climate. The microstructure described here is very similar to that of Retallack (1991), thus we interpret it originated at an early stage in soil formation.

4.3. La Perra locality (site 3 of Fig. 1C)

The section of altered sediments is 90 cm thick; including the upper 2–3 cm thick of crusted surface. The sediments are completely disturbed and no primary stratification is recognized in the first 25 cm. After that and down the profile some slight relict stratification becomes evident. This site presents similar features to Simbolar; the distinctive ones are: bioturbation, mottling, root traces and dolomite precipitation gradational (Fig. 6D and E). No horizonation is visible. The section presents grading color changes from the uppermost level characterized by moderate red color 5R 5/4, to pale reddish brown (10R 5/4) and grayish red (10R 4/2) down profile to pale purple (5P 6/2) and pale green (10G 6/2) in the unaltered sediments.

The crusted surface is characterized by desiccation cracks and bioturbation. Bioturbation consists of simple vertical tubes many centimeters long and 5–4 mm wide, and are interpreted as product of animal activity.

Downward the profile in the dark reddish brown zone, circular greenish-gray drab halos 5–6 mm in diameter are distinctive. Horizontal fractures filled with calcite also occur. This latter feature presents identical characteristics as in Simbolar.

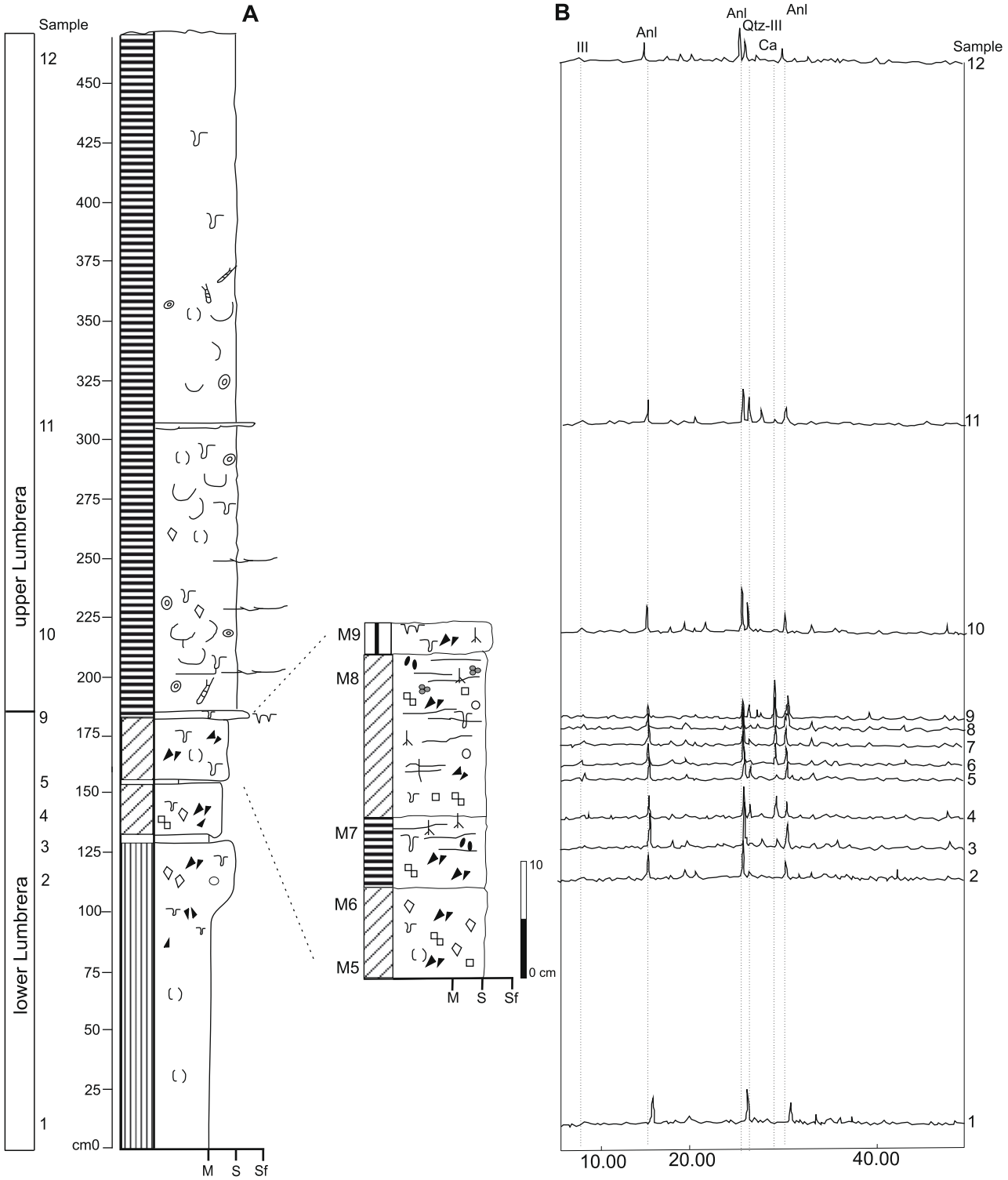

Fig. 5. (A) Simbolar detail log showing the main sedimentological and pedologic characteristics of the paleosurface. (B) Stratigraphic variation in mineralogical composition and relative abundance from XR diffractometry.

We sampled seven levels encompassing unaltered through altered indurated levels of lower Lumbrera to unaltered sediments of the overlying upper Lumbrera units (Fig. 6D).

Petrography reveals an asepic (argillasepic) microfabric and the presence of numerous channels, both vertical and horizontal. Channels are coated with Fe-oxides and clays and infilled with peloidal mudstones and disseminated calcite crystals.

As shown in Fig. 6E the main minerals are analcime, calcite and hematite. Calcite is present as patches of microsparite and mosaic of sparite and crystal rhombs disseminated in the fine-grained groundmass or/and filling voids. Illite is the dominant clay, but significant amounts of smectite occur in two of the sampled levels.

5. Geochemical characteristics

Many authors have investigated chemical changes produced by weathering (e.g. Nesbitt, 1979; Nesbitt and Young, 1982; Nesbitt

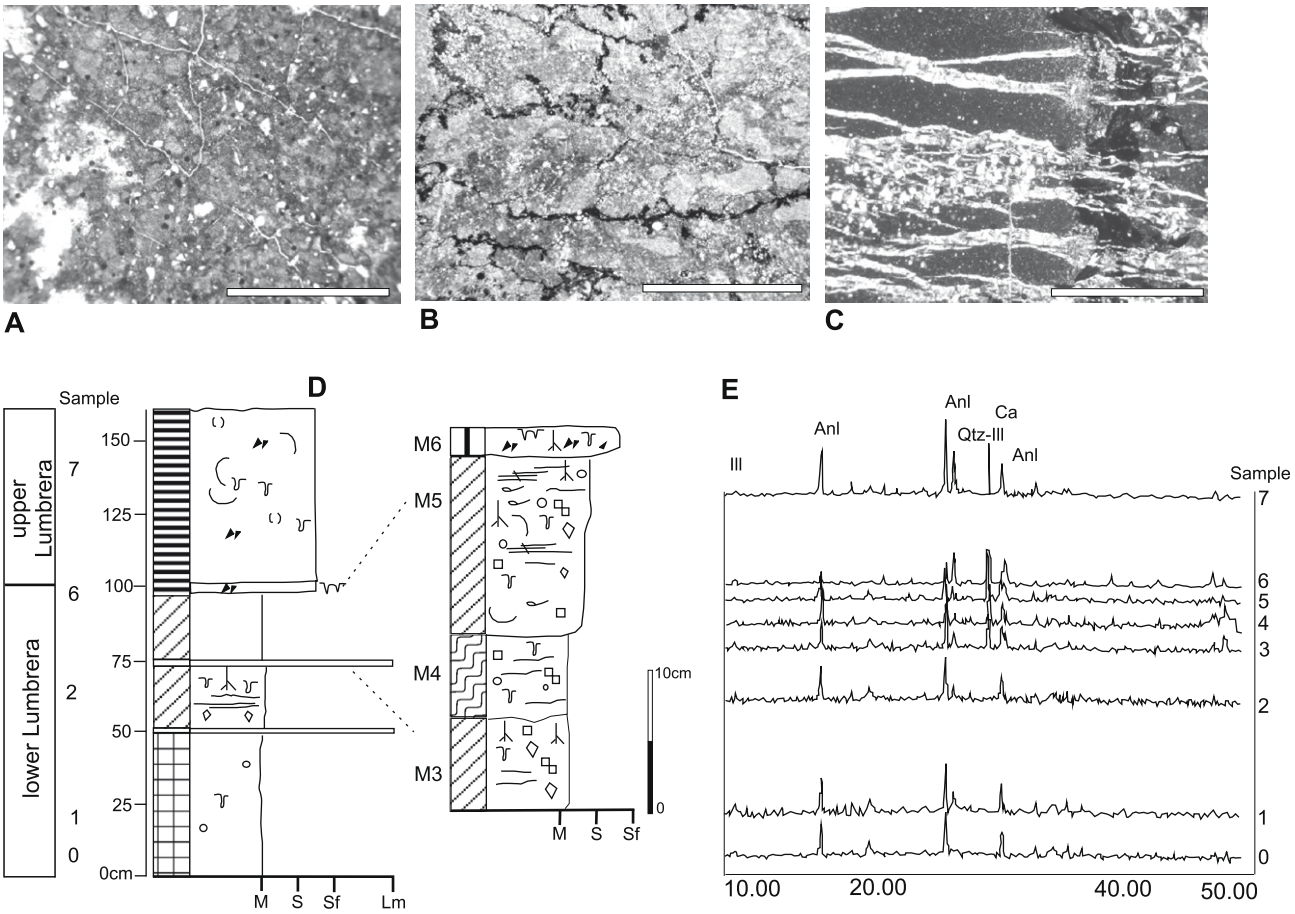

Fig. 6. (A) Micritic clotted textures and disseminated irregular calcite glaebulas, La Perra, (plane light). (B) Iron oxides filling voids between incipient granular peds, Simbolar (crossed polarized light) (C) Horizontal fractures filled with displacive sparry calcite and disseminated rhombohedric calcite, Simbolar, (crossed polarized light). Scale bar for the three photographs is 1 mm. (D) La Perra detail log showing the main sedimentological and pedologic characteristics. (E) Stratigraphic variation in mineralogical composition and relative abundance from XR diffractometry.

and Young, 1989; Nesbitt and Markovics, 1997). The Chemical Index of Alteration (CIA), proposed by Nesbitt and Young (1982), is a widely used method for establishing the intensity of weathering in sediment source areas and in soils. The index is calculated as (using molar proportions):

$$\mathrm{CIA} = [\mathrm{A_2O_3}/(\mathrm{Al_2O_3} + \mathrm{CaO^*} + \mathrm{Na_2O} + \mathrm{K_2O})]100$$

where $\mathrm{CaO^*}$ represents the CaO contained in silicates only. In our case, the protolith for the altered horizon is already the result of a previous weathering process, i.e. pelitic sediment. Furthermore, the studied profiles contain variable amounts of diagenetic carbonate and phosphate-bearing fossil materials, which would all have an impact on the CIA formula and may be difficult to correct for properly.

The correction for the calcium contained in apatite is relatively straightforward if apatite is the only phosphate present. In this work, we assume this to be true, and correct for phosphate-related CaO by stoichiometry using $\mathrm{P_2O_5}$ data from chemical analysis. However, the presence of samples with high LOI and CaO content, together with petrographic and mineralogical information, indicates that carbonate (mostly calcite) is a major calcium host in the studied profiles. Since $\mathrm{CO_2}$ was not independently determined in this study, we could not correct for carbonate-hosted CaO directly. McLennan (1993) suggests a method for CaO correction in the absence of direct $\mathrm{CO_2}$ determination, by evaluating the relative molar proportions of CaO (after correction for apatite) and $\mathrm{Na_2O}$. In that case, when the number of CaO moles is less than that of $\mathrm{Na_2O}$, the CaO molar proportion is adopted as the $\mathrm{CaO^*}$ value. Otherwise, the molar proportion of $\mathrm{CaO^*}$ is considered to be equivalent to that of $\mathrm{Na_2O}$.

Our attempts at applying CIA to compare altered and unaltered rocks in the profiles, even considering the corrections proposed by McLennan (1993), failed to yield results that were consistent with petrographic and mineralogical observations. Fig. 7 compares the CaO, LOI, and corrected CIA values; it is clear that the CIA values are still affected by the presence of carbonate. As predicted by McLennan (1993), calculations where the $\mathrm{CaO^*}$ correction is based on molar $\mathrm{Na_2O}$ yield only minimum CIA values. In our case, because the starting materials are already the product of weathering, the CIA in the altered zone decreases rather than increases. As suggested by Bloch et al. (2006), this could be due to reverse weathering (i.e. diagenesis and/or contact metamorphism), but, apart from the formation of diagenetic carbonate, there is no direct chemical or mineralogical evidence to support this hypothesis. For instance, although CaO increases in the weathered profile due to carbonate precipitation, all other CIA oxides ($\mathrm{Al_2O_3}$, $\mathrm{Na_2O}$, $\mathrm{K_2O}$) actually decrease in that horizon (see Fig. 7).

The right-hand side diagram in Fig. 7 shows a modified form of the chemical index of alteration, disregarding CaO entirely, as suggested by Gravina et al. (2002). The values for feldspar and illite are plotted for comparison. The little variation observed in the molar $\mathrm{Al_2O_3}/(\mathrm{Al_2O_3} + \mathrm{Na_2O} + \mathrm{K_2O})$ ratio indicates that chemical leaching was not extensive in any of the three studied weathering profiles, suggesting that paleosol formation occurred under a relatively dry climate. Therefore, for the cases reported here, this simpler form of

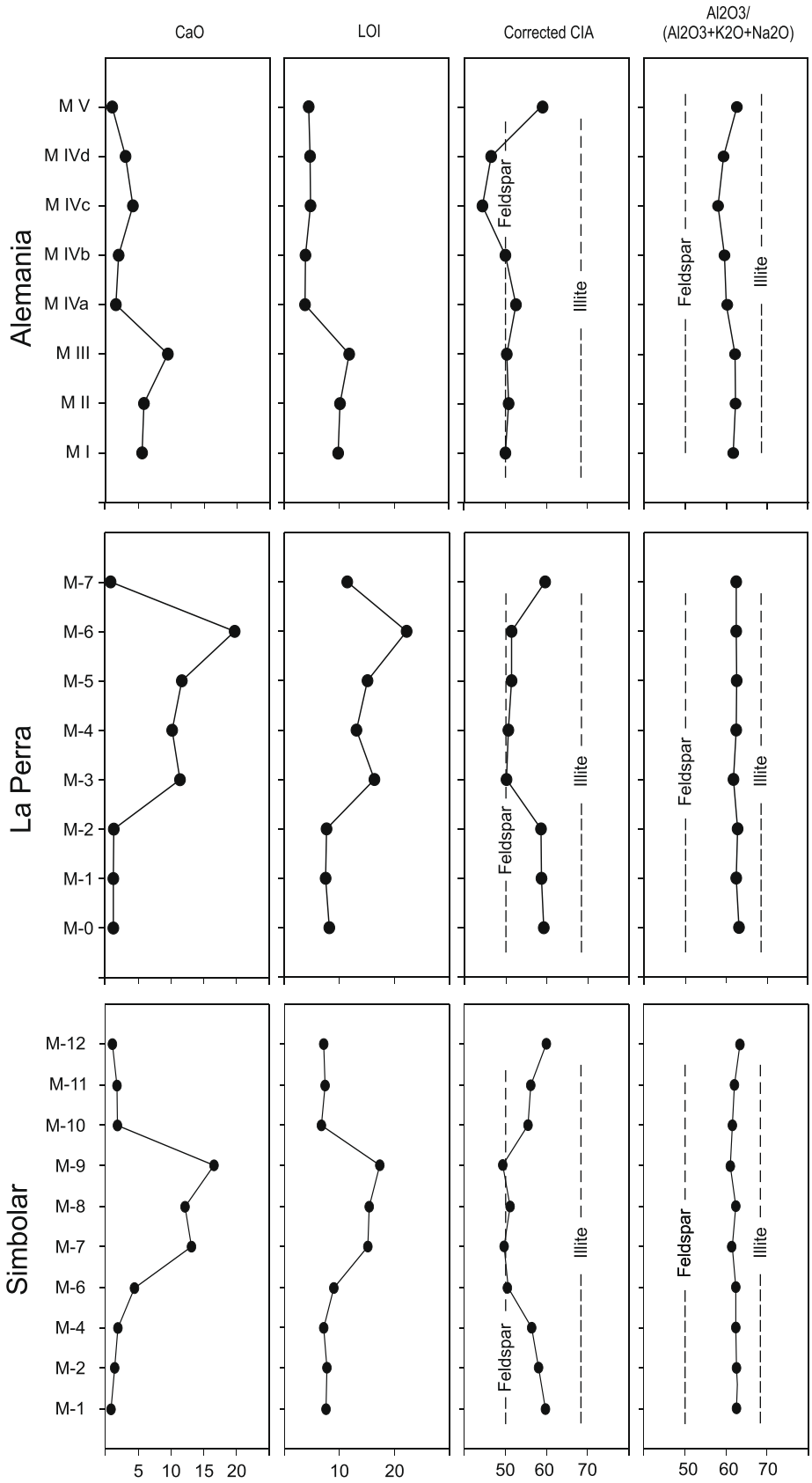

Fig. 7. Behavior of CaO, LOI, CIA and CIA modified $Al_2O_3/(Al_2O_3 + Na_2O + K_2O)$ in the three profiles. Values for feldspars and illite are plotted for comparison. Note that CIA values are still affected by the carbonate-rich passages.

the alteration index produces the most consistent results, while still providing a reasonable estimate of the degree of weathering both in the source areas and sedimentary rocks, and in soil and paleosol profiles.

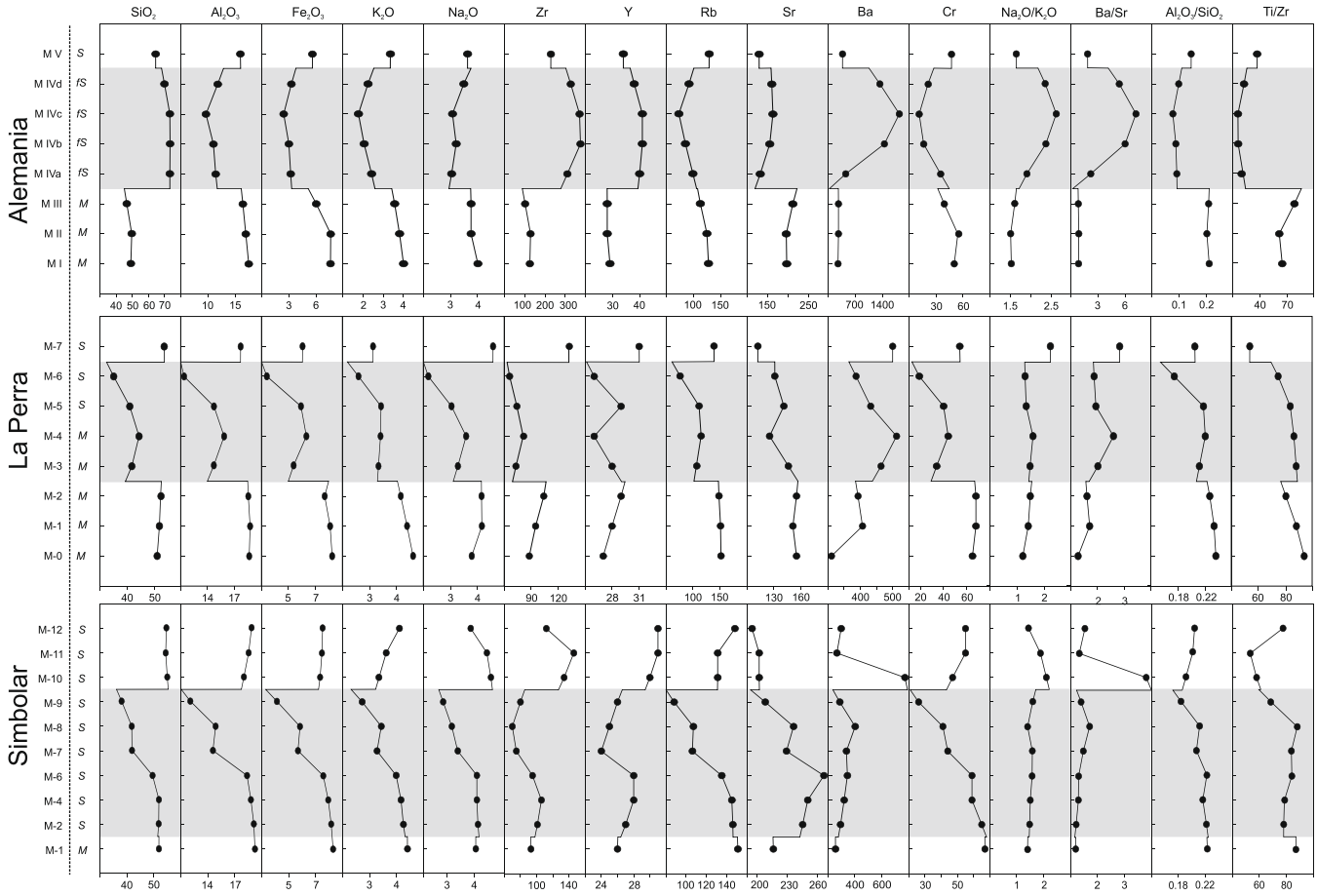

Fig. 8. Chemical variations in selected major and minor elements and molar ratios in the three profiles. Inflection points in the curves highlight the top and/or the base of the hardened weathering horizon. Grayish area represents weathered level. Italic capital letters indicates the textural composition of each sample (see Fig. 2 for key).

Detailed chemical variations may be best observed when the original geochemical data and molar ratios are plotted as profiles (Fig. 8). Inflection points in the curves of many major and trace elements highlight the top and/or base of hardened weathering horizons. Overall, the profiles at La Perra and Simbolar are similar, whereas the Alemania profile shows distinctive characteristics.

At the base of the weathering level in the Alemania profile, there is an increase in the SiO_2 content, corresponding to the high concentration of quartz grains recognized in petrography (Fig. 8). This suggests that the SiO_2 increase may be partly due to a more sandy character of the original sediment towards the top of the Alemania sequence (Fig. 2E – IVd). On the other hand, this locality contains the best-developed paleosols among all the studied profiles, which is consistent with silica enrichment. Al_2O_3, Fe_2O_3, Na_2O, K_2O (Fig. 8), and CaO (Fig. 7) all decrease in the altered level at Alemania. P_2O_5 (not shown) behaves in the same way as Al_2O_3. While alkalis and calcium behave as expected during weathering, reflecting hydrolyzation and leaching of the more soluble cations, the decrease in Fe_2O_3 and Al_2O_3 cannot be easily explained. It may be a side (closed-sum) effect of the strong SiO_2 enrichment, or the result of local physical–chemical conditions (see below). Zr and Y increase sympathetically in the altered horizon, indicating residual zircon concentration. Nb (not shown) behaves in the same way as Zr and Y. Rb follows the behavior of K, and Sr accompanies Ca, since these are common substituting cations in minerals. Ba shows a very strong increase in the weathered horizon, ranging from ca. 250 ppm in the original sediment to up to 1800 ppm in the upper-middle part of the weathered horizon. Cr and (not shown) Ni and V are depleted in the weathered horizon.

Molar ratios are often used to assess alteration processes during weathering (e.g. Retallack, 1997). At Alemania, the Al_2O_3 to SiO_2 molar ratio signals an increase in quartz proportions relative to clay minerals, observed in thin section. The Ti/Zr ratio is also lower in the weathered horizon, probably due to higher zircon concentration. More importantly, Ti/Zr suggests a different provenance for the sediments below and above the weathered profile. Ba/Sr is generally interpreted as a measure of chemical leaching (Retallack, 1997, 2004), but at Alemania this is not supported by the Al to alkalis molar ratio (Fig. 7). Moreover, since the magnitude of Ba enrichment in the weathered horizon is expressive, we suggest that the high Ba/Sr values observed in this profile result from sulphate precipitation, since barite was observed in thin sections and confirmed in SEM analysis.

We interpret barite precipitation as having happened during paleosol formation under a relatively dry climate, which agrees well with the sympathetic increase in the salinization Na_2O/K_2O ratio (Fig. 8).

At the La Perra and Simbolar localities, the starting (parent) materials are more clayey than at Alemania, with implications for the chemistry of the weathering horizon. Also, in both sections, there is marked precipitation of calcite in the upper portions of this level that is not so pronounced at Alemania.

At La Perra (Fig. 8), SiO_2, Al_2O_3, K_2O, Na_2O, and Fe_2O_3 behave sympathetically in the weathered profile, showing a sharp decrease at the bottom, followed by a slight increase, and then a progressive decrease towards the top. CaO (see Fig. 7) behaves in an opposite way, in response to the precipitation of calcite veinlets, visible in outcrop and thin section. The joint depletion in silica,

iron, aluminum and alkalis could perhaps be assigned to a closed-sum effect related to calcite enrichment, similar to that involving quartz enrichment at Alemania. Here, however, progressive increases in molar Al_2O_3/SiO_2 and Ti/Zr from top to bottom of the weathered profile indicate an increasing abundance of clay minerals, probably resulting from clay infiltration during paleosol formation. Furthermore, Ti/Zr values below and above the weathered horizon suggest a change in provenance. Zr contents are lower in the weathering profile than in the starting materials and remain approximately constant in this horizon, increasing sharply again in the overlying pelites. Contrary to Alemania, Zr and Y variations show some discrepancy within the weathered horizon, suggesting that the Y distribution is not entirely controlled by zircon. Sympathetic behavior between Y and (not shown) P_2O_5 and Th suggests that the Y distribution at La Perra is at least partially controlled by phosphate. Rb varies sympathetically with K_2O. Sr, on the other hand, does not follow the CaO distribution, suggesting that Sr is not strongly controlled by carbonate precipitation. Although the Ba composition range is much narrower than at Alemania, Ba shows a similar pattern of enrichment in the middle part of the La Perra weathered profile. Cr (Ni and V, not shown) is marginally lower in the weathering horizon than in the parent materials, showing more intense depletion at both its top and bottom. A relatively constant Na_2O/K_2O molar ratio suggests that salinization was not significant at La Perra.

At Simbolar (Fig. 8), SiO_2, Al_2O_3, and Fe_2O_3 show general depletion in the weathered horizon, relative to the starting materials. As in La Perra, a general downward increase in molar Al_2O_3/SiO_2 suggests an accumulation of migrating clay minerals at the bottom half of the weathering profile. The upward CaO increase in the profile is consistent with the presence of calcite veinlets at the top. Similar to La Perra, there is no correlation between CaO and Sr. In the bottom half of the altered zone, Zr, Y, and (not shown) Nb contents are similar to those observed in the unaltered material below, but all three elements are depleted in the upper half. Cr and (not shown) Ni behave sympathetically, decreasing gradually from bottom to top of the altered zone. Molar Ba/Sr indicates moderate leaching in the upper half section of the paleosol, and molar Na_2O/K_2O indicates that salinization was not a significant process at Simbolar.

Iron is depleted at the top and concentrated at the bottom of the weathered horizon in all three localities. The presence of abundant root marks at the upper level of the paleosol suggests that the system was enriched in organic matter and could have developed adequate redox conditions for the downward migration of reduced Fe^{2+}. Below this hypothesized reduced level, iron would have precipitated as Fe^{3+} and concentrated in lower levels (Fig. 4F). Aluminum behavior is consistent with soil-forming processes, and may be explained through clay-mineral migration and accumulation at the bottom half of the profile, particularly in the cases of La Perra and Simbolar.

Molecular ratios of relatively inert geochemical indicators have been used in many studies to help locate discontinuities in soils and paleosols (Al-Gailani, 1980; McCarthy and Plint, 2003). Ti and Zr are found in minerals that are resistant to alteration and therefore tend to accumulate as weathering progresses. In uniform parent materials, Ti/Zr should change gradually and uniformly with depth, without sharp inflections or reversals in trends (McCarthy and Plint, 2003). At the Alemania profile (Fig. 8), a strong inflection in this ratio marks the passage, below the surface, of unaltered materials to altered ones (hardened level), which may be a feature partly inherited from an original Zr-enriched sandy material, further enhanced by pedogenic processes. It is noteworthy that this feature is absent or incipient at La Perra and Simbolar (Fig. 8).

The strong enrichment in SiO_2 (Alemania) and CaO (La Perra and Simbolar) raises the question of how many of the described features are actually produced by paleosol-forming processes, and how many are the result of closed-sum effects, particularly regarding the major elements.

Mass fluxes between different portions of chemical weathering and soil forming systems are particularly useful monitors of near

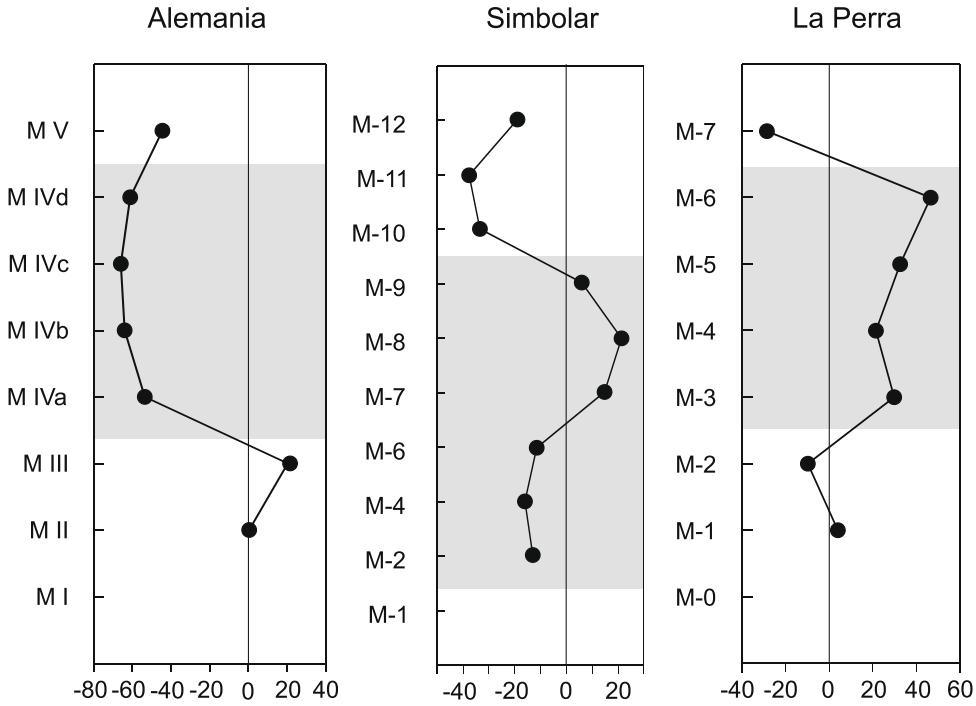

Fig. 9. Strain $\varepsilon_{Zr,w}$ plotted against depth for each profile. Positive values show dilation and negative values show collapse (see text for explanation). Grayish area represents weathered level.

surface transport processes. Because mass fluxes in soils are computed from mass conservation volume–density (ρ)-compositions relation, it is imperative to evaluate the effects of volume change. Recent improvement in the physiochemical strain gauge based on mass balance has allowed to determine the amount and sense of deformation in soils and therefore to use the accumulated strain to calculate chemical gains and losses (Brimhall et al., 1991). These authors define strain as:

$$\varepsilon_{i,w} = \rho_p C_{i,p}/\rho_w C_{i,w} - 1 \quad (1)$$

Positive strains are dilations and negative strains represent collapse. Collapse is indicated when the concentration of an immobile element ($C_{i,w}$) caused by loss of mobile constituents is not exactly compensated by an inversely proportional decrease in bulk density (ρ_w) due to increasing porosity such that the product of $C_{i,w}$ and ρ_w remains constant.

Once the bulk strain is computed with Eq. (1), absolute chemical mass gains and losses per unit of volume of parent material, $\delta_{j,w}$, are calculated with Eq. (2) (Brimhall et al., 1991):

$$\delta_{j,w} = m_{j,\mathrm{flux}}/\mathbf{V}_p = [\rho_w C_{j,w}(\varepsilon_{i,w} + 1) - \rho_p C_{j,p}]/100 \quad (2)$$

In Alemania, the negative strain observed at all sampled depths shows that this section of the weathered horizon is dominated by collapse (Fig. 9), which is typical of more developed or aged soils (Brimhall et al., 1991). This particularity is indicated also in Fig. 8, where the concentrations of immobile Zr are increased in the weathered level.

At Simbolar and La Perra, positive strain values indicate expansion, which is consistent with physical brecciation observed in outcrops and hand specimen, and the infilling of open fractures with carbonate. In these cases, the observed decrease in the absolute concentration of immobile Zr (Fig. 8) may be explained by dilution. Furthermore, the La Perra profile is dominated by expansion, with a very slightly developed collapse zone at its bottom. On the other hand, the Simbolar profile shows a well defined division, whereby the lower half is dominated by collapse and the upper half is dominated by expansion.

Brimhall et al. (1991) state that soils evolve from dilation to collapse as they mature. In that sense the strain profiles in Fig. 9 suggest that the sequence La Perra – Simbolar – Alemania represents a continuum of progressively more evolved soil profiles.

6. Paleosurface: interpretation and meaning

The presence of a paleosol is demonstrated by the recognition of root traces, soil horizons and, features like sepic plasmic microfabrics (Retallack, 1988). The identification of a paleosol in the Alemania, La Perra and Simbolar sites, distant from one another (Fig. 1C), allows us to interpret this paleosol as a regional feature.

Vegetation grew over the desiccated lake surface, altering and oxidizing the silty parent material. The predominant reddish color and the identification of ferrans suggest well-oxygenated soils. Moreover the presence of granular structures, ferruginous glaebules, and sepic plasmic fabric are indicative of weathering and leaching of the soluble and suspended material of the upper levels and their accumulation in lower positions, determining eluvial and illuvial pedogenic horizons, respectively (Fig. 3F).

Furthermore, the geochemical evidence pinpoints the weathered level in all three profiles. Inflection points in the curves of many major and trace elements highlight the top and/or the base of the hardened weathering horizon (Fig. 8). Overall, the profiles at La Perra and Simbolar are chemically similar, whereas the distinctive characteristics of Alemania result from a more sandy character of the protolith combined with a higher degree of soil evolution. The consistent behavior of Al, Mg, Fe, K and Ti suggests destabilization and hydrolysis of biotite at the weathering surface. Iron is depleted at the top and concentrated at the bottom of the weathered horizon in all three localities, which is interpreted as a result of remobilization and secondary precipitation. Al behavior is consistent with soil-forming processes, and may be explained through clay-mineral migration and accumulation at lower levels, particularly in the cases of La Perra and Simbolar. The geochemical evidence indicates similar evolution patterns for the La Perra and Simbolar profiles. The differences observed at Alemania are due to the combined effects of (a) a more sandy character of the original sediment towards the top of the sequences, and (b) a higher degree of soil profile evolution, with predominance of collapse processes.

We applied a modified form of the chemical index of alteration (Fig. 7). The little variation observed in molar $Al_2O_3/(Al_2O_3 + Na_2O + K_2O)$ indicates that chemical leaching was not extensive in any of the three weathering profiles. This index gives a reasonable estimate of the degree of weathering (interpreted as intermediate) in both the source areas and the sedimentary rocks.

Differentiation of the horizons allows an assessment of the relative degree of maturity of the paleosols (Retallack, 1988). We recognized moderately developed paleosols in Alemania to weakly developed paleosols at Simbolar and an even less mature profile at La Perra. The differences in soil maturity reflect differences in the rate of pedogenic factors, such as local paleo-relief variations or differences in residence times over which the processes operated (Curtis, 1990; Wright, 1989).

It is significant to note that the sedimentological features, the Na_2O/K_2O ratio and the overall weathering imprints converge to suggest that paleosol formation occurred under a temperate and relatively dry climate and a probable local increase in salinization.

The features described here and the interpreted geological processes that affected this horizon lead us to interpret it as a sedimentary discontinuity. Furthermore, the variation in the Ti/Zr ratios below and above the weathered horizon, which suggests a change in provenance for the sedimentary protolith, constitutes additional evidence that the studied horizons represent discontinuities in the sedimentary record in the region.

The time involved in this discontinuity is uncertain, but if we consider the geochemical imprints and sedimentological features, there is no evidence of prolonged exposure. Thus, we interpret this paleosurface as an omission surface (Bromley, 1975) that represents a minor break in the sedimentary column marking a temporary halt in deposition involving little or no erosion (Bromley, 1975). Such minor breaks in sedimentation are typically intraformational, but interformational surfaces without large-scale erosion also exist.

7. Dating the discontinuity

Although dating the paleosurface is currently beyond our capability, paleontological evidence and the first radiometric ages obtained for the upper Lumbrera Formation provide some insight into the age of the omission surface.

7.1. Radiometric age

In the Pampa Grande area (Fig. 1C), the upper Lumbrera Formation is 274 m thick. Toward the top, a continuous white 25 cm-thick layer of crystal-tuff (Fig. 2A), composed of plagioclase, biotite, quartz, and zircon was identified. We used zircon crystals for radiometric age dating.

The calculated age is 39.9 ± 0.4 Ma (Fig. 10); errors for isotopic ratios shown in Tables 1 are 2σ.

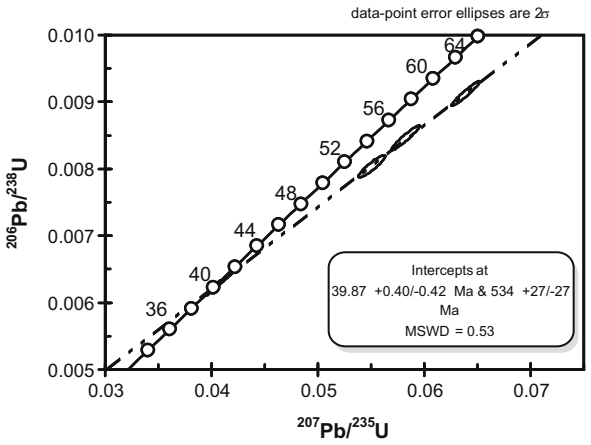

Fig. 10. $^{206}Pb/^{238}U$ vs. $^{207}Pb/^{235}U$ correlation diagram for zircon concentrate from upper Lumbrera tuff, Simbolar.

7.2. Paleontology

Most of the vertebrate fossils found in the Lumbrera Formation come from the Pampa Grande region (Fig. 1C) (e.g. Carbajal et al., 1977; Vucetich and Bond, 1982; Bond and López, 1993; Babot et al., 2002; Pascual, 1980a,b; Deraco et al., 2008), which is one of the most important paleontological locations for this unit.

The discontinuity identified is also evident in the mammalian fossil associations; none of the known genera of fossil mammals recorded for the lower Lumbrera Formation persists into upper Lumbrera strata. In the upper Lumbrera deposits, mammals are relatively abundant and well preserved mainly big herbivores. Basal leontiniids and the campanorcid *Campamanorco inauguralis* (Bond et al., 1984) were found in these levels. However the mammal association, although different in composition does not reflect a strong climatic or environmental change.

Leontiniids include Coquenia bondi (Deraco et al., 2008) and at least another taxon represented by incomplete specimens, some of them articulated. Leontiniids have been previously reported from two other localities in northwestern Argentina: close to the confluence of the Casa Grande and Laguna rivers (Jujuy Province), Casa Grande Formation (Bond and López, 1995), and Cerro Bayo, close to La Poma (Salta Province), Quebrada de los Colorados Formation (Hongn et al., 2007). The peculiar notoungulate *Campamanorco inauguralis* is interpreted as a basal typothere (Reguero et al., 1996). It is characterized by an advanced dental pattern that anticipates the model established in the advanced Typotheria. Another undescribed taxon found in the same strata shows similar dental specializations.

Finally, a conspicuous Dasypodidae was found in the upper Lumbrera at Río Juramento, 54 km N-NE of Simbolar. The pattern of the dermal scutes of this armadillo clearly differs from all known dasypodids due to the presence of three high longitudinal ridges of the anterior articular surface of the mobile scutes (Herrera and Powell, 2007). These peculiar dasypodid dermal plates were also found in the Casa Grande Formation, close to the confluence of the Casa Grande and Laguna rivers (Jujuy Province).

In order to highlight the contrasting paleontological record below and above the omission surface, we listed the main tetrapods registered in both lower and upper Lumbrera Formation.

7.2.1. List of fossil tetrapods of the lower Lumbrera

The fossils included in this list were found at Pampa Grande area (Fig. 1C).

Order Crocodylia
  Family Sebecidae
    cf. *Sebecus*
Order Squamata
  Family Teiidae
    Lumbrerasaurus scagliai (Donadío, 1985)
Infraorder Sparssodonta
  SuperFamily Borhyaenoidea
  Family Proborhyaenoidae
    Callistoe vincei (Babot et al., 2002)
    Borhyaenoidea indet. (Babot, 2005)
Order Polydolopimorphia
  Family Bonapartheriidae
    Bonapartherium hinakusijum (Pascual, 1980b)
  Family Prepidolopide
    Prepidolops didelphoides (Pascual, 1980a)
    Prepidolops molinae (Pascual, 1980a)
Order Astrapotheria
  Family Astrapotheriidae
    Albertogaudrya? carahuensis (Carbajal et al., 1977)
Orden Litopterna
  Family Adianthidae
    Indalecia grandensis (Bond and Vucetich, 1983)
Order Notoungulata
  Family Notoylopidae
    Boreastylosps lumbrerense (Vucetich, 1980)
  Family Isotemnidae
    Pampatemnus infernalis (Vucetich and Bond, 1982)
    Pampatemnus deuteros (Vucetich and Bond, 1982)
  Family Oldfieldtomasiidae
    Colbertia lumbrerense (Bond, 1981)
  Family Notohippidae
    Pampahippus arenalesi (Bond and López, 1993)

7.2.2. List of fossil tetrapods of the upper Lumbrera

All the mammals found in these levels were located within the first 50 m above the weathering surface at Simbolar, except the dasypodid material found at Río Juramento. They are usually well preserved, many articulated but incomplete because of present-day removal and erosion, but without significant evidence of transport.

Table 1
Summary of U–Pb data for upper Lumbrera ash layer. (*) Commmon Pb corrected using measured ^{204}Pb. (**) Million year error for individual fraction.

Sample fraction	Size (mg)	U (ppm)	Pb (ppm)	Th (ppm)	Th/U (ppm)	Pb 206 Pb204 (obs.)	Pb207* U235	(pct)	Pb206* U238	(pct)	Correl. Coeff. (rho)	Pb207* Pb206*	(pct)	Pb206* U238 Age	Pb207* U235 Age	Pb207* Pb206* Age	Ma.**
Lum. F	0.222	328.84	3.052	720.8	2.19194745	434.9212	0.0550611	1.86	0.00803549	1.69	0.913876	0.0496971	0.753	51.593	54.423	180.85	18
Lum. H	0.318	219.32	2.02	503.2	2.2943644	441.9793	0.0582401	1.88	0.0084647	1.800	0.956629	0.0524947	0.549	51.663	57.478	307.03	13
Lum. J	0.205	355.53	3.61	780.6	2.19559531	544.2857	0.0639053	1.73	0.009128	1.660	0.963057	0.0507760	0.465	58.576	62.899	230.67	11
Lum. G	0.345	287.65	3.765	450.5	1.56613941	655.2340	0.0402	1.34	0.00622	1.45	0.976	0.0468500	0.233	39.973	40.019	41.59	1
Lum. I	0.356	345.21	4.023	654.4	1.896	435.3440	0.04115	1.56	0.00634	1.34	0.99	0.0472100	0.256	40.741	40.946	59.863	1

Order Xenarthra
Family Dasypodidae
Dasypodidae new genus and sp. (Herrera and Powell, 2007)
Order Notoungulata
Family Leontiniidae
Coquenia bondi Deraco et al., 2008
Leontinidae indet. (new genus?)
Family Olfieldtomsiidae
Dolichostylodon saltensis (García López and Powell, 2009)
Family Campanorciidae
Campanorco cf. inauguralis Bond and Vucetich, 1983
Family Isotemnidae
Isotemnidae indet.

Although the fossil association of the upper Lumbrera is still poorly known in terms of diversity, the first appearance of basal members of the family Leontiniidae marks an important milestone in the evolution of South American notoungulates. These basal leontiniids are found in stratigraphic units overlying the weathering surface in the Lerma valley. The presence of the relatively advanced notoungulate *Campanorco,* absent in the lower Lumbrera deposits, is consistent with the evidence suggested by the leontiniid fossils.

7.3. Age discussion

The occurrence in the same profile of Simbolar of a rich vertebrate fauna, the dating of the tuff and the omission surface offer an opportunity to analyze the age of the Lumbrera Formation and, not being our main goal, to discuss it in the context of the mammal biostratigraphy for first time in northwestern Argentina, which is a matter of constant debate.

Traditionally, the Lumbrera Formation has been assigned to the "Casamayoran" South American Land Mammal Age (SALMA), i.e. Early Eocene (Carbajal et al., 1977; Pascual, 1980a Pascual, 1980b; Pascual et al., 1981; Bond and Vucetich, 1983). This age estimate was based mainly on the "volutionary grade"of the mammal association registered in the lower Lumbrera deposits, which is similar to that of the "Casamayoran" SALMA in Patagonia. However there are no common species or even genera between these distant regions.

Absolute age dates for the Casamayoran are extremely scarce and controversial. Conventionally, this SALMA was referred to the early Eocene (Pascual et al., 1965; Marshall et al., 1983). Ciffeli (1985) proposed two divisions for the "Casamayoran" Vacan and Barrancan (Fig. 11).

If this Patagonia framework is extrapolated to the Lumbrera Formation in northwestern Argentina, the lower Lumbrera could be more or less coeval to the Vacan (Fig. 11), while the upper Lumbrera, as confirmed by our absolute age, chronologically equivalent to the Barrancan SALMA.

On the other hand, Sempere et al. (1997) based on magnetostratigraphic studies of the Lumbrera Formation, have interpreted the top of the section, i.e. "lower Lumbrera" in the Pampa Grande region, as ~ 54.5 Ma (almost the Paleocene-Eocene boundary). This interpretation is clearly not supported by our paleontological and stratigraphic evidence.

Recent research (Vucetich et al. 2007; López, personal communication) has updated the chronological interpretation of South American mammal ages and indicate a Middle Eocene age for the Vacan and Barrancan (Fig. 11). In this framework, upper Lumbrera can be chronologically correlated to the Barrancan, while lower Lumbrera corresponds likely to the Vacan SALMA, although there is not absolute dating for lower Lumbrera.

In summary, the paleontological record suggests a Middle Eocene age for the lower Lumbrera (Lutetian) and Late Lutetian-Early Bartonian for the upper Lumbrera, the latter being in accordance with our 39.9 Ma U/Pb zircon determination. This evidence points to a Middle Eocene (Lutetian) age for the discontinuity described here.

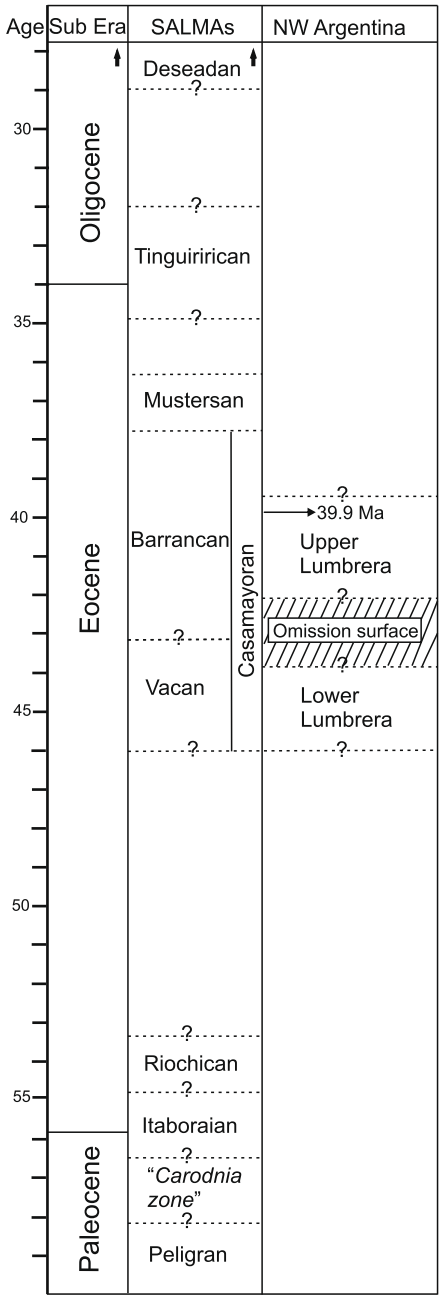

Fig. 11. Adapted South American Land Mammal ages for the Lumbrera Formation (see text for explanation).

8. Eocene basin evolution: discussion and conclusions

The multidisciplinary approach applied to the Lumbrera indurated surface resulted in a useful tool for recording discontinuity surfaces, in particular for recognizing paleosurfaces for which field expressions are obscure. Our centimeter by centimeter logs allowed us to recognize slight sedimentological and geochemical variations, showing the weathering processes that affected the sedimentary level. The sedimentological and geochemical characteristics of the indurated surface and the distinction of different

paleoenvironments and vertebrate fossil associations below and above it document the presence of an omission surface.

If we consider the regional geological context of the Eocene in northwestern Argentina, some interesting insights emerge from the recognition of this omission surface and its importance in reconstructing basin evolution.

The Paleogene records the beginning of Central Andean uplift, documented by variable deformation, magmatic activity and sedimentation, mainly in continental basins (Sébrier et al., 1988; Tawackoli et al., 1996; Baby et al., 1997; Benavídez Cáceres, 1999; Kraemer et al., 1999; Hartley et al., 2000; Mpodozis et al., 2005; Carrapa et al., 2005). The recognition of an intra-Lumbrera Formation omission surface and the new radiometric dating allow for a better definition of the age and basin evolution of this unit. The Middle Eocene is a crucial time in the Central Andes, recording the age of initial crustal thickening, uplift of Paleozoic granites in Bolivia (Benjamin et al., 1987), magmatic and tectonic activity in the Cordillera de Domeyko in Chile (Coira et al., 1993; Richards et al., 2001; Mpodozis et al., 2005) and exhumation and mountain formation in the Puna-Altiplano (Haschke et al., 2005; DeCelles et al., 2007).

In the Puna-Eastern Cordillera transition (NW – Argentina), del Papa et al. (2004) and Hongn et al. (2006) documented a compressive tectonic event and syntectonic sedimentation in the Middle Eocene Quebrada de los Colorados Formation, located in the Calchaquí Valley, to the west of the studied Lumbrera Formation (Fig. 1B). In that area, the Quebrada de los Colorados Formation is overlying by local angular unconformity the Salta post-rift deposits and preserves growth-strata structures recording the beginning of Andean sedimentation (Hongn et al., 2007). The vertebrate fossils of the Quebrada de los Colorados Formation are comparable to the fossil associations of the upper Lumbrera Formation, particularly the common presence of Notoungulata and Leontiniidae (Hongn et al., 2007). In addition, the characteristics of the facies association – thick red siltstone beds intercalated with minor sandy channels facies – particularly in the lower part of both units, are common. Therefore, the radiometric age, the paleontological record and the sedimentological attributes allow us to interpret Quebrada de los Colorados and upper Lumbrera as proximal and distal sedimentological expressions of the same sedimentary basin, so their are correlatives and, consequently, the unconformity of their basal contact. Our data and interpretation confirm the previous proposal of Starck and Vergani (1996).

Hence, we can synthesize the Middle Eocene basin scenario considering the following geological statements: (1) the presence of Middle Eocene basal angular unconformity and syntectonic sedimentation in the Valle Calchaquí and eastern Puna (Hongn et al., 2007 and Carrapa and DeCelles, 2008; Payrola Bosio et al., 2006); (2) presence of Middle Eocene omission surface in the Lerma valley approximately 70 km eastward of the fault-fold zone (restoration considering a shortening of nearly 15%, Coutand et al., 2001); (3) both Quebrada de los Colorados and upper Lumbrera formations present basal thick red fine-grained alluvial plain deposits and shallow lakes; (4) these units contain the same vertebrate fossil association, which substantially differs from the Salta rift vertebrate record.

There are more questions than facts regarding the distribution of Eocene deformation and sedimentation in this part of the Central Andes. However, the omission surface described in this paper represents undoubtedly a zone of Eocene "tectonic quiescence". Based on the conceptual models of Andean evolution in which deformation and sedimentation propagate in the foreland direction (i.e. Jordan and Alonso, 1987; Carrapa and DeCelles, 2008), the Puna-Eastern Cordillera transition (Fig. 1B) may be interpreted as the easternmost Eocene deformation front, considering the lack of well-defined Eocene deformation features to the east. In this context, the omission surface recognized in the La Perra, Simbolar and Alemania sections represents areas in which deformation vanished from the western deformation front (Fig. 12A). Available data make this interpretation the more sustainable one.

However, there are other features that allow alternative interpretations, as they suggest that the Eocene deformation front was eastward of the Eastern Cordillera-Puna transition. One of these is the west-vergence of faults related to Middle Eocene deformation-sedimentation (Puna, see DeCelles et al., 2007; Calchaquí Valley, see Hongn et al., 2007). If the first episodes of rift-related fault inversion took place during the Middle Eocene as proposed by Hongn et al. (2007), and inverted normal faults splay from a deeper east-vergent thrust (Grier et al., 1991), a Middle Eocene first-order east-vergent fault should exist eastward of the Calchaquí Valley, probably in the Metán area (Fig. 12B), as Allmendinger et al. (1982) and Mon (2001), among others,

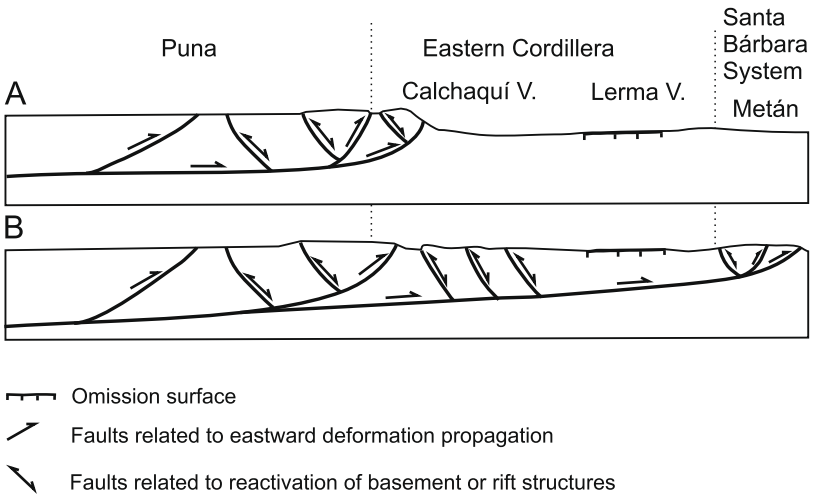

Fig. 12. West–east cross-section schemes showing two probable alternative models for explaining the Lerma valley omission surface. (A) The Puna-Eastern Cordillera transition defines the easternmost expression of Eocene deformation, so the omission surface represents the distal foreland basin. (B) The Eocene deformation front is eastward of the Lerma valley. The omission surface represents a zone of tectonic quiescence between the deformation zone and the back-thrust formed by tectonic inversion of the normal Cretaceous faults. Not to scale.

interpreted for Neogene deformation. In this way, the alternative interpretation of the La Perra-Simbolar-Alemania omission surface as a tectonic quiescence zone between two regions of Eocene deformation should be considered a feasible hypothesis that needs further revisions in key areas that can preserve evidence of Eocene deformation-sedimentation (Fig. 12B).

Available data are still scarce and do not allow a definitive interpretative model. However the omission surface described here is a new evidence of the discontinuities molded in basin shifts, representing the beginning of the foreland basin sedimentation and offers a new puzzle piece for reconstructing the distribution of Eocene deformation and related sedimentation in northwest Argentina.

Acknowledgments

This work was funded by ANPCyT (PICT 2006-381), CONICET (PIP 5255), and is part of the international cooperative program Secyt/Capes N° BR/PA05/UVII014. We thank Tim White, Randall Marrett and Luis Buatois for useful discussions on aspects of an earlier draft of the manuscript; we also thank Guillermo López for his advisement in relation to the chronology of South American Land Mammal Ages and to Ricardo Pereyra and Nilda Menegatti for XRF and XRD laboratory assistance. Reviews by D. Starck and an anonymous referee greatly improved this contribution. We thank U. Riller for revision of the original English of the manuscript.

References

Al-Gailani, M.B., 1980. Geochemical identification of unconformities using semi-quantitative X-ray fluorescence analysis. Journal of Sedimentary Petrology 50 (4), 1261–1270.

Allen, P.A., Allen, J.R., 1990. Basin Analysis. Principles & Applications. Blackwell Scientific Publication, Oxford. pp. 459.

Allmendinger, R., Jordan, T., Palma, R., Ramos, V., 1982. Perfil estructural en la Puna catamarqueña (25–27°), Argentina. V Congreso Latinoamericano de Geología, Argentina. Proceedings, Buenos Aires, vol. 1. pp. 499–518.

Babot, M.J., 2005. Los Borhyaenoidea (Mammalia, Metatheria) del Terciario Inferior del Noroeste Argentino. Aspectos filogentéticos, paleobiológicos y bioestratigráficos. Ph.D. Thesis, Facultad de Ciencias Naturales e Instituto Miguel Lillo, Universidad Nacional de Tucumán, Argentina.

Babot, M.J., Powell, J.E., De Muizon, C.H., 2002. Callistoe vincei, a new proborhyaenidae (Borhyeanoidea, Metatheria, Mammalia) from the early Eocene of Argentina. Geobios 35, 615–629.

Baby, P., Rochat, P., Mascle, G., Hérail, G., 1997. Neogene shortening contribution to crustal thickening in the back arc of the Central Andes. Geology 25, 883–886.

Benavídez Cáceres, V., 1999. Orogenic evolution of the Peruvian Andes: the Andean cycle. In: Skinner, B. (Ed.), Geology and Ore Deposits of the Central Andes, Chapter 3. Society of Economic Geologist, Special Publication 7, pp. 61–107.

Benjamin, M.T., Johnson, N.M., Naeser, C.W., 1987. Recent rapid uplift in the Bolivian Andes: evidence from fission-track dating. Geology 15, 680–683.

Birkeland, P.W., 1984. Soils and Geomorphology. Oxford University Press, New York, pp. 372.

Bloch, J.D., Timmons, J.M., Crossey, L.J., Gehrels, G.E., Karlstrom, K.E., 2006. Mudstone petrology of the mesoproterozoic Unkar Group, Grand Canyon, USA: provenance, weathering, and sediment transport on intracratonic Rodinia. Journal of Sedimentary Research 76, 1106–1119.

Boll, A., Hernández, R., 1986. Interpretación estructural del área de Tres Cruces: Boletín de Informaciones Petroleras. Tercera Epoca, III (7), 2–14.

Bond, M., 1981. Un nuevo Oldfieldthomasiidae (Mammalia, Notoungulata) del Eoceno inferior (Fm. Lumbrera, Grupo Salta) del NW argentino. II Congreso Latinoamericano Paleontología (P. Alegre, 1981). Anais 2, 521–536.

Bond, M., López, G., 1993. El primer Notohippidae (Mammalia, Notoungulata) de la formación Lumbrera (Grupo Salta) del noroeste argentino. Consideraciones sobre la sistemática de la familia Notohippidae. Ameghiniana 30, 59–68.

Bond, M., López, G., 1995. Los Mamíferos de la Formación Casa Grande (Eoceno) de la Provincia de Jujuy, Argentina. Ameghiniana 32, 301–309.

Bond, M., Vucetich, M.G., 1983. Indalecia grandesis gen. et sp. nov. del Eoceno temprano del Noroeste Argentino, tipo de una nueva subfamilia de los Adianthidae (Mammalia, Litopterna). Revista de la Asociación Geológica Argentina 37, 107–117.

Bond, M, Vucetich, M.G., Pascual, R., 1984. Un nuevo Notoungulata de la Formación Lumbrera (Eoceno) de la Provincia de Salta, Argentina. I Jornadas Argentinas de Paleontología de Vertebrados, Proceedings, pp. 20.

Brewer, R., 1976. Fabric and Mineral Analysis of Soils. Krieger, New York. pp. 482.

Brimhall, G.H., Chadwick, O.A., Lewis, C.J., Compston, W., Williams, I.S., Danti, K.J., Dietrich, W.E., Power, M.E., Hendricks, D., Bratt, J., 1991. Deformational mass transport and invasive processes in soil evolution. Science 255, 695–702.

Bromley, R.G., 1975. Trace fossils at omission surfaces. In: Frey, R.W. (Ed.), The Studies of Trace Fossils. Springer-Verlag, New York, pp. 399–428.

Cahill, T., Isacks, B.L., 1992. Seismicity and shape of the subducting Nazca Plate. Journal of Geophysical Research 97, 17503–17529.

Carbajal, E., Pascual, R., Pinedo, R., Salfity, J., Vucetich, M.G., 1977. Un Nuevo Mamífero de la Formación Lumbrera (Grupo Salta) de la Comarca de Carahuasi (Salta, Argentina). Edad y Correlaciones. Publicaciones del Museo Municipal de Ciencias Naturales de Mar del Plata "Lorenzo Scaglia" 2, Mar del Plata, vol. 7, pp. 148–163.

Carrapa, B., DeCelles, P., 2008. Eocene exhumation and basin development in the Puna of northwestern Argentina. Tectonics 27, TC1015. doi:10.1029/2007TC002127.

Carrapa, B., Adelmann, D., Hilley, G., Mortimer, E., Sobel, E., Strecker, M., 2005. Oligocene range uplift and development of plateau morphology in the southern central Andes. Tectonics 24, TC4011. doi:10.1029/2004TC001762.

Carrera, N., Muñoz, J., 2008. Thrusting evolution in the southern Cordillera Oriental (northern Argentine Andes): constraints from growth strata. Tectonophysics 459 (1/4), 107–122.

Carrera, N., Muñoz, J., Sàbat, F., Mon, R., Roca, E., 2006. The role of inversion tectonics in the structure of Cordillera Oriental (NW Argentinean Andes). Journal of Structural Geology 28, 1921–1932.

Catuneanu, O., 2004. Retroarc foreland systems – evolution through time. Journal of African Earth Sciences 38, 225–242.

Ciffeli, R.L., 1985. Biostratigraphy of the Casamayoran, Early Eocene, of Patagonia. Novitates. American Museum of Natural History, New York, vol. 2820, pp. 1–26.

Coira, B., Mahlburg, Kay, S., Viramonte, J., 1993. Upper Cenozoic magmatic evolution of the argentine Puna – a model for changing subduction geometry. International Geology Review 35 (8), 677–720.

Coutand, I., Cobbold, P., de Urreiztieta, M., Gautier, P., Chauvin, A., Gapais, D., Rossello, E., López Gamundi, O., 2001. Style and history of Andean deformation, Puna plateau, northwestern Argentina. Tectonics 20 (2), 210–234.

Coutand, I., Carrapa, B., Deeken, A., Schmitt, A., Sobel, E., Strecker, M., 2006. Propagation of orographic barriers along an active range front: insights from sandstone petrography and detrital apatite fission-track thermochronology in the intramontane Angastaco basin, NW-Argentina. Basin Research 18, 1–26.

Curtis, C.D., 1990. Aspects of climatic influence on the clay mineralogy and geochemistry of soils, palaesols and clastic sedimentary rocks. Journal of the Geological Society of London 147, 351–357.

DeCelles, P., Giles, A., 1996. Foreland basin systems. Basin Research 8, 105–123.

DeCelles, P., Carrapa, B., Gehrels, G., 2007. Detrital zircon U–Pb ages provide provenance and chronostratigraphic information from Eocene synorogenic deposits in northwestern Argentina. Geology 35, 323–326.

del Papa, C.E., 2006. Estratigrafía y Paleoambientes de la Formación Lumbrera, Grupo Salta, Noroeste Argentino. Revista Asociación Geológica Argentina 61 (3), 15–29.

del Papa, C.E., Hongn, F.D., Petrinovic, I.A., Domínguez, R., 2004. Evidencias de deformación pre-miocena media asociada al antepaís andino en la Cordillera Oriental (24°35′S–66°12O′). Asociación Geológica Argentina Revista 59 (3), 506–509.

Deraco, V., Powell, J., Lopez, G., 2008. Primer leontínido (Mammalia, Notoungulata) de la Formación Lumbrera (Subgrupo Santa Bárbara, Grupo Salta) del Noroeste Argentino. Ameghiniana 45 (1), 83–91.

Donadío, O.E., 1985. Un nuevo lacertilio (Squamata, Sauria, Teiidae) de la Formación Lumbrera (Eoceno Temprano) Provincia de Salta, Argentina. Ameghiniana 22 (3/4), 221–228.

Echavarría, L., Hernández, R., Allmendinger, R., Reynolds, J., 2003. Subandean thrust and fold belt of northwestern Argentina: Geometry and timing of the Andean evolution. American Association of Petroleum Geologists, 965–985.

Esteban, M., Klappa, C., 1983. Subaerial exposure environment. In: Scholle, P.A., Bebout D.G., Moore, C.H. (Eds.), Carbonate Depositional Environments. American Association of Petroleum Geologist, Memoir, vol. 33, pp. 1–54.

Ettensohn, F.R., Dever, G.R. Jr., Grow, J.S., 1988. A paleosols interpretation for profiles exhibiting subaerial exposure "crust" from the Mississippian of the Appalachian Basin. Geological Society of America, Special Paper 216, pp. 49–80.

Fleming, P.B., Jordan, T.E., 1989. A synthetic stratigraphic model of foreland basin development. Journal of Geophysical Research 94 (B4), 3851–3866.

Galli, C., Hernández, R., 1999. Evolución de la cuenca de antepaís desde la zona de la Cumbre Calchaquí hasta la Sierra de Santa Bárbara, Eoceno inferior – Mioceno medio, provincia de Salta, Argentina. In: Colombo, F., Querault, I., Petrinovic, I. (Eds.), Geología de los Andes Centrales Meridionales: El Noroeste Argentino. Acta Geológica Hispánica 34(2–3), pp. 167–184.

García López, D.A., Powell, J.E., 2009. Un Nuevo Oldfieldthomasiidae (Mammalia:Notoungulata) del Paleógeno de la provincia de Salta, Argentina. Ameghiniana 46 (1), 153–164.

Gómez Omil, R.J., Boll, A., Hernández, R.M., 1989. Cuenca cretácico-terciaria del Noroeste argentino (Grupo Salta). In: Chebli, G.A., Spalletti, L.A. (Eds.), Cuencas Sedimentarias Argentinas. Universidad Nacional de Tucumán, Serie de Correlación Geológica, vol. 6. Tucumán, pp. 43–64.

Gravina, E.G., Kafino, C.V., Brod, J.A., Boaventura, G.R., Santos, R.V., Guimarães, E.M., Jost, H., 2002. Proveniência de arenitos das Formações Uberaba e Marília (Grupo Bauru) e do Garimpo do Bandeira: implicações para a controvérsia sobre a fonte do diamante do Triângulo Mineiro. Revista Brasileira de Geociências 32 (4), 545–558.

Grier, M.E., Salfity, J.A., Allmendinger, R.W., 1991. Andean reactivation of the Cretaceous Salta rift, northwestern Argentina. Journal of South American Earth Sciences 4 (4), 351–372.

Hartley, A., May, G., Chong, G., Turner, P., Kape, S., Jolley, E., 2000. Development of a continental forearc: a Cenozoic example from the Central Andes, northern Chile. Geology 28, 331–334.
Haschke, M., Deeken, A., Insel, N., Grove, M., Smichtt, A., 2005, Growth pattern of the Andean Puna plateau constrained by apatite (U/Th)/He, K-feldspar 40Ar/39Ar, and zircon U–Pb geochronology. VI International Symposium on Andean Geodynamics (ISAG 2005) Extended Abstracts, Barcelona, pp. 360–363.
Hasiotis, S., Mitchell, C., 1993. A comparison of crayfish burrow morphologies: triassic and Holocene fossil, paleo- and neo-ichnological evidence, and the identification of their burrowing signature. Ichnos 2, 291–314.
Hernández, R., Galli, C., Reynolds, J., 1999. Estratigrafía del Terciario en el Noroeste Argentino. Relatorio. XIV Congreso Geológico Argentino, Proceedings, Salta, vol. 1, pp. 316–328.
Herrera, C.M., Powell, J.E., 2007. Un peculiar armadillo (Xenarthra, Dasypodidae) del Paleógeno del Noroeste argentino. Su valor cronoestratigráfico. XXI Jornadas Argentinas de Mastozoología, Proceedings, vol. 1, pp. 246–247.
Hongn, F., del Papa, C., Petrinovic, I., Mon, R., Powell, J., 2006. Sedimentación sintectónica en la base del Grupo Payogastilla (¢Paleógeno?-Neógeno), Valle Calchaquí norte, Salta. Asociación Geológica Argentina, Publicación Especial Serie D N10, pp. 84–90.
Hongn, F., del Papa, C., Powell, J., Petrinovic, I., Mon, R., Deraco, V., 2007. Middle Eocene deformation and sedimentation in the Puna-Eastern Cordillera transition (23–26°S): control by preexisting heterogeneities on the pattern of initial Andean shortening. Geology 35 (3), 271–274.
Hongn, F, Mon, R., Petrinovic, I., del Papa, C., Powell, J., 2008. Inversión tectónica en el noroeste argentino: influencia de las heterogeneidades del basamento. XVII Congreso Geológico Argentino, Proceedings, San Salvador de Jujuy, p. 25.
Horton, B., 1998. Sediment accumulation on top of the Andean orogenic wedge: oligocene to late Miocene basins of the Eastern Cordillera, southern Bolivia. Geological Society of America Bulletin 110 (9), 1174–1192.
Horton, B., DeCelles, P., 1997. The modern foreland basin system adjacent to the Central Andes. Geology 25 (10), 895–898.
Jordan, T., 1981. Thrust loads and foreland basin evolution, cretaceous, Western United States. Amercian Association Petroleum Geologists Bulletin 65 (12), 2506–2520.
Jordan, T., Allmendinger, R., 1986. The Sierras Pampeanas of Argentina: a modern analogue of Rocky Mountain foreland deformation. American Journal of Science 286, 737–764.
Jordan, T., Alonso, R., 1987. Cenozoic stratigraphy and basin tectonics of the Andes Mountains, 20–28 South latitude. American Association of Petroleum Geologist Bulletin 71 (1), 49–64.
Jordan, T., Schlunegger, F., Cardozo, N., 2001. Unsteady and spatially variable evolution of the Neogene Andean Bermejo foreland basin, Argentina. Journal of South American Earth Sciences 14, 775–798.
Kley, J., 1998. Structural styles of foreland deformation in the Andes. Zeitschrift der Deutschen Geologischen Gesellschaft 149 (1), 13–26.
Kraemer, B., Adelman, D., Akten, M., Schnurr, W., Erspentein, K., Kiefer, E., van den Bogaard, P., Görler, K., 1999. Incorporation of the paleogene foreland into neogene Puna plateau: the Salar de Antofalla area, NW Argentina. Journal of South American Earth Sciences 12, 157–182.
Krogh, T.E., 1973. A low-contamination method for hydrothermal decomposition of zircon and extraction of U and Pb for isotopic age determinations. Geochimica et Cosmochimica Acta 37, 485–494.
Ludwig, K.R., 1993. PBDAT. A computer program for processing PB–U–Th isotope data. USGS Open File Report 88-544, pp. 34.
Ludwig, K.R., 2001. Users Manual for Isoplat/Ex version 2.47. A geochronological toolkit for Microsoft Excel. Berkeley Geochronology Center. Special Publication 1a, pp.55.
Marquillas, R., del Papa, C., Sabino, I., 2005. Sedimentary aspects and paleoenvironmental evolution of a rift basin: Salta Group (Cretaceous-Paleogene), northwestern Argentina. International Journal of Earth Sciences 94 (1), 94–113.
Marshall, L.G., Hoffstetter, R., Pascual, R., 1983. Mammals and stratigraphy: Geochronology of the continental mammal-bearing Tertiary of South America. Paleovertebrata, mémoire extraordinaire, pp. 1–93.
McCarthy, P.J., Martini, I.P., Leckie, D.A., 1999. Pedogenic and diagenetic influences on void coating formation in Lower Cretaceous paleosols of the Mill Creek Formation, southwestern Alberta, Canada. Geoderma 87, 209–237.
McCarthy, P.J., Plint, G.A., 2003. Spatial variability of paleosols across Cretaceous interfluves in the Dunvegan Formation, NE British Columbia, Canada: paleaohydrological, palaeogeomorphological and stratigraphic implications. Sedimentology 50, 1187–1220.
McLennan, S.M., 1993. Weathering and global denudation. Journal of Geology 101, 295–303.
Mon, R., 2001. Estructuras curvadas y levantamientos verticales en la Cordillera Oriental (prov. Salta y Tucumán). Revista de la Asociación Geológica Argentina 56, 367–376.
Monaldi, R., Salfity, J., Vitulli, N., Ortiz, A., 1993. Estructuras de crecimiento episódico en el subsuelo de la laguna de Guayatayoc, Jujuy, Argentina. XII Congreso Geológico Argentino, Proceedings, Mendoza, vol. 3, pp. 55–64.
Mortimer, E., Carrapa, B., Countand, I., Schoenbohm, L., Sobel, E., Sosa Gomez, J., Strecker, M., 2007. Fragmentation of a foreland basin in response to out-of-sequence basement uplifts and structural reactivation: El Cajón-Campo Arenales basin, NW Argentina. Geological Society of America Bulletin 119 (5/6), 637–653.
Mpodozis, C., Arriagada, C., Basso, M., Roperch, P., Cobbold, P., Reich, M., 2005. Late mesozoic to paleogene stratigraphy of the Salar de Atacama Basin, Antofagasta, Northern Chile: implications for the tectonic evolution of the Central Andes. Tectonophysics 399, 125–154.
Nesbitt, H.W., 1979. Mobility and fractionation of rare earth elements during weathering of a granodiorite. Nature 279, 206–210.
Nesbitt, H.W., Young, G.M., 1982. Early proterozoic climates and plate motions inferred from major element chemistry of lutites. Nature 299, 715–717.
Nesbitt, H.W., Young, G.M., 1989. Formation and diagenesis of weathering profiles. Journal of Geology 97, 129–147.
Nesbitt, H.W., Markovics, G., 1997. Weathering of granodioritic crust, long-term storage of elements in weathering profiles, and petrogenesis of siliciclastic sediments. Geochimica et Cosmochimica Acta 61 (8), 1653–1670.
Pascual, R., 1980a. Prepidolopidae, una nueva familia de Marsupialia didelphoidea del Eoceno sudamericano. Ameghiniana 17, 216–242.
Pascual, R., 1980b. Nuevos y singulares tipos ecológicos de marsupiales extinguidos de América del Sur (Paleoceno Tardío o Eoceno temprano) del Noroeste Argentino. II Congreso Argentino de Paleontología y Bioestratigrafía y I Congreso Latinoamericano de Paleontología, Proceedings, Buenos Aires, vol. 2, pp. 151–173.
Pascual, R., Ortega Hinojosa, E.D., Gondar, D., Tonni, E., 1965. Las edades del Cenozoico mamalífero de la Argentina, con especial atención a aquellas del territorio bonaerense. Comunicación Investigación Científica, Proceedings, Buenos Aires, vol. 6, pp. 165–193.
Pascual, R., Bond, M., Vucetich, M., 1981. El Subgrupo Santa Bárbara (Grupo Salta) y sus vertebrados, cronología, paleoambientes y paleobiogeografía. VIII Congreso Geológico Argentino, Proceedings, vol. 3, pp. 743–778.
Payrola Bosio, P.A., Powell, J., Hongn, F. del Papa, C., 2006. Registro de deformación eocena en el Valle de Luracatao, noroeste del Valle Calchaquí. XII Reunión de Tectónica. Proceedings, San Luis, p. 47.
Reguero, M.A., Bond, M., López, G.M., 1996. Campanorco inaguralis: an approach to the phylogeny of the Typotheria. Journal of Vertebrate Paleontology 15(Suppl. 3), 59A.
Reichenberger, V., 2004. Numerical Simulation of Multiphase Flows in Fractured Porous Media. Ph.D. Thesis (Unpublished). Naturwissenschaftlich-Mathematichen Gesamtfakultät der Ruprecht-Karls, Universität Heidelberg, pp. 149.
Retallack, G.J., 1988. Field recognition of paleosols. In: Reihardt, J., Sigleo, W. (Eds.): Paleosols and weathering through geologic time: principles and applications. Geological Society of America, Special Paper 216, pp. 1–20.
Retallack, G.J., 1991. Miocene Paleosols and Ape Habitats of Pakistan and Kenya. Natural Sciences Library. Oxford University Press, Clarendon Press (pp. 323).
Retallack, G.J., 1997. Neogene expansion of the North American prairie. Palaios 12, 380–390.
Retallack, G.J., 2004. Late Oligocene bunch grassland and early Miocene sod grassland paleosols from central Oregon, USA. Palaeogeography, Palaeoclimatology, Palaeoecology 207, 203–237.
Reynolds, J., Galli, C., Hernández, R., Idleman, B., Kotila, J., Hilliard, R., Naeser, C., 2000. Middle Miocene tectonic development of the Transition Zone, Salta province, northwest Argentina: magnetic stratigraphy from the Metán Subgroup, Sierra de González. Geological Society of America Bulletin 112 (11), 1736–1751.
Richards, J., Boyce, A., Pringle, M., 2001. Geologic evolution of the Escondida area, Northern Chile: a model for spatial and temporal localization of porphyry cu mineralization. Economic Geology 96, 271–305.
Riller, U., Hongn, F., 2003. Structural significance of Paleozoic discontinuities on Cretaceous to Quaternary tectonism in the eastern Cordillera, NW-Argentina. Geophysical Research Abstracts, 5.
Sabino, I.F., 2004. Estratigrafía de la Formación La Yesera (Cretácico): Base del relleno sinrift del Grupo Salta, noroeste argentino. Revista de la Asociación Geológica Argentina 59 (2), 341–359.
Salfity, J.A., 1982. Evolución Paleogeográfica del Grupo Salta (Cretácico-Eogénico), Argentina. V CongresoLatinoamericano de Geología, Proceedings, vol. 1, Buenos Aires, pp. 11–26.
Salfity, J.A., Marquillas, R.A., 1994. Tectonic and Sedimentary evolution of the cretaceous-eocene salta group basin, Argentina. In: Salfity, J.A. (Ed): Cretaceous Tectonics of the Andes. Earth Evolution Sciences, Friedr. Vieweg & Sohn, pp. 266–315.
Schlagintweit, O., 1936. Los insectos fósiles del Norte Argentino y la edd de Horizonte Calcáreo Dolomítico. Noticia Preliminar. Boletín de Informaciones Petroleras 13 (145), 61–69.
Sébrier, M., Lavenu, A., Fornari, M., Soulas, J.P., 1988. Tectonics and uplift in Central Andes (Perú, Bolivia and Northern Chile) from Eocene to present. Geodynamique 3 (1/2), 85–106.
Sempere, T., Butler, R.F., Richards, D.R., Marshall, L.G., Sharp, W., Swisher III, C.C., 1997. Stratigraphy and chronology of upper cretaceous-lower paleogene strata in Bolivia and northwest Argentina. Geological Society of America Bulletin 109 (6), 709–727.
Sinclair, H.D., Coakley, B.J., Allen, P.A., Watts, A.B., 1991. Simulation of foreland basin stratigraphy using a diffusion model of mountain belts uplift and erosion: and example from the Central Alps, Switzerland. Tectonics 10 (3), 599–620.
Starck, D., Vergani, G., 1996. Desarrollo tectosedimentario del Cenozoico en el sur de la provincia de Salta. XIII Congreso Geológico Argentino, Proceedings, vol. 1, Buenos Aires, pp. 433–452.
Tawackoli, S., Jacobshagen, V., Wemmer, K., Andriessen, P.A.M., 1996. The Eastern Cordillera of southern Bolivia: a key region to the Andean backarc uplift and

deformation history. III International Symposium on Andean Geodynamics (ISAG 1996), Extended Abstracts, Saint Malo, pp. 505–508.
Teruggi, M.E., Andreis, R.R., 1971. Micromorphological recognition of paleosolic features in sediments and sedimentary rocks. In: Yaalon, D.H. (Ed.), Paleopedology – Origin, Nature and Dating of Paleosols. Instl. Soc. Soil Sciences and Israel Universities Press, pp. 161–171.
Vergani, G., Starck, D., 1989. Aspectos estructurales del Valle de Lerma al sur de la ciudad de Salta. Boletín de Informaciones Petroleras 20, 2–9.
Vucetich, M.G., 1980. Un nuevo Notostylopidae (Mammalia, Notoungulata) proveniente de la Formación Lumbrera (Grupo Salta) del Noroeste Argentino. Ameghiniana 17 (4), 363–372.
Vucetich, M.G., Bond, M., 1982. Los primeros Isotemnidae (Mammalia, Notoungulata) registrados en la Formación Lumbrera (Grupo Salta), del Noroeste Argentino. Ameghiniana 19, 7–18.
Vucetich, M.G., Reguero, M.A., Bond, M., Candela, A.M., Carlini, A.A., Deschamps, C.M., Gelfo, J.N., Goin, F.J., López, G.M., Ortiz Jaureguizar, E., Pascual, R., Schillato Yané, G.J., Vieytes, E.C., 2007. Mamíferos continentales del Paleógeno argentino: las investigaciones de los últimos cincuenta años. Ameghiniana 50° Aniversario. Special Publication 11, pp. 239–255.
Wright, V.P., 1989. Paleosol recognition. In: Allen, J.R.L., Wright, V.P. (Eds.), Paleosols in siliciclastic sequences. Postgraduate Research Institute for Sedimentology, Reading University. Short Course Notes N°001, pp. 1–25.